Automaton Constrained Q-Learning

Anastasios Manganaris, Vittorio Giammarino, and Ahmed H. Qureshi
Department of Computer Science
Purdue University
{amangana,vgiammar,ahqureshi}@purdue.edu

Abstract

Real-world robotic tasks often require agents to achieve sequences of goals while respecting time-varying safety constraints. However, standard Reinforcement Learning (RL) paradigms are fundamentally limited in these settings. A natural approach to these problems is to combine RL with Linear-time Temporal Logic (LTL), a formal language for specifying complex, temporally extended tasks and safety constraints. Yet, existing RL methods for LTL objectives exhibit poor empirical performance in complex and continuous environments. As a result, no scalable methods support both temporally ordered goals and safety simultaneously, making them ill-suited for realistic robotics scenarios. We propose Automaton Constrained Q-Learning (ACQL), an algorithm that addresses this gap by combining goal-conditioned value learning with automaton-guided reinforcement. ACQL supports most LTL task specifications and leverages their automaton representation to explicitly encode stage-wise goal progression and both stationary and non-stationary safety constraints. We show that ACQL outperforms existing methods across a range of continuous control tasks, including cases where prior methods fail to satisfy either goal-reaching or safety constraints. We further validate its real-world applicability by deploying ACQL on a 6-DOF robotic arm performing a goal-reaching task in a cluttered, cabinet-like space with safety constraints. Our results demonstrate that ACQL is a robust and scalable solution for learning robotic behaviors according to rich temporal specifications.

1 Introduction

Achieving desirable robot behavior in real-world applications often requires managing long and complex sequences of subgoals while adhering to strict safety constraints. For instance, autonomous mobile robots in warehouse settings must navigate to restock shelves, all while avoiding obstacles and remaining within a reachable distance from the recharging station for their current battery level. Similarly, a nursing robot must routinely complete its rounds in a given sequence, unless notified of an emergency situation.

Despite the success of Goal-Conditioned Reinforcement Learning (GCRL) [1, 2] and Safe RL [3, 4], these approaches fall short in addressing the combined challenges of sequential goals and dynamic safety constraints. GCRL is effective for reaching individual goals but lacks mechanisms for reasoning over goal sequences or ensuring safety. Safe RL enforces fixed safety constraints, but typically assumes they remain static throughout the task, limiting its applicability to temporally evolving tasks.

Formal languages such as LTL [5] provide an expressive framework for specifying complex tasks involving multiple interdependent goals and non-stationary safety constraints. However, reward functions defined directly from LTL specifications are inherently non-Markovian, since temporal properties refer to entire trajectories rather than individual transitions. This violates the Markov assumption—a fundamental premise of standard RL—which assumes that transitions and rewards

39th Conference on Neural Information Processing Systems (NeurIPS 2025).

depend only on the current state and action. As a result, RL algorithms built on the Markov Decision Process (MDP) formalism [6, 7] are ill-suited for direct application to LTL-defined objectives.

To overcome this, some studies [8–10] have proposed to translate the LTL formula into an automaton that tracks temporal progress toward task completion and enables defining Markovian rewards corresponding to temporal specifications. While this approach allows for potentially handling arbitrary LTL formulas, its generality is tied to the use of sparse binary rewards derived from the Boolean evaluation of the specification. In complex environments, however, such sparse signals are encountered too infrequently to effectively guide behavior, and designing denser rewards typically requires additional domain knowledge not readily available in many robotics tasks. Furthermore, these methods only implicitly deal with ensuring safety, as safety properties are fundamental components of many LTL specifications [11], and typically rely on ad-hoc mechanisms, such as halting rollouts [12] and reward shaping [13], both of which tend to be brittle and ineffective in complex domains. Other approaches seek to improve scalability by employing hierarchical [13] or goal-conditioned [14] policies but sacrifice generality, particularly with respect to safety constraints.

To bridge the gap between LTL-capable algorithms that scale poorly and scalable RL algorithms that lack support for most LTL tasks, we propose ACQL, which lifts Safe RL and GCRL to the class of problems expressible as LTL formulae in the recurrence class [15]. This algorithm, which we consider our primary contribution, is built on top of two technical novelties that address distinct challenges associated with LTL problems. First, to overcome the poor scalability of sparse rewards, we encode automaton states with their associated goals, enabling the use of goal-conditioned techniques such as Hindsight Experience Replay (HER) [2] to densify reward signals. Second, inspired by Hamilton-Jacobi (HJ) reachability analysis [16, 17], we employ a minimum-safety-based product Constrained Markov Decision Process (CMDP) formulation that enforces compliance with arbitrary LTL safety constraints at optimality. We demonstrate these technical contributions are necessary in enabling our ACQL algorithm to significantly outperform other algorithms for solving LTL tasks. Additionally, we demonstrate its effectiveness in learning real-world-deployable policies for a 6-DOF robot arm operating in a storage cabinet environment.

2 Related Work

The use of LTL specifications with RL algorithms has been a popular topic in recent years [10, 13, 18–28]. One approach to this topic has been directly defining non-Markovian reward functions based on overall task satisfaction, but this only supports LTL formulae that are satisfiable over finite prefixes [18, 29–31]. In restricted cases where task satisfaction is differentiable with respect to a policy's actions, it is also possible to directly train sequence models that satisfy the specification [23]. The most popular and general methods, however, convert LTL tasks into automata to use in conjunction with standard deep RL techniques for MDPs [8–10, 19, 22, 24–28, 32–36]. Within these works, there are two subcategories including methods for learning policies that can perform well across a set of multiple LTL tasks [20, 22, 25, 27] and methods that focus on optimally satisfying a single LTL task [8–10, 12, 19, 28, 32, 36, 37].We specifically aim to improve on the scalability of these latter methods in high-dimensional environments. Of these techniques, we specifically highlight Reward Machines (RMs) [37] as a framework with similar generality to our method and the first baseline we compare against.

Our work utilizes techniques from GCRL [38, 39] to accelerate learning for LTL tasks. Other methods have taken a related approach by learning or re-using goal-conditioned policies that are hierarchically guided by LTL expressions to enable zero-shot generalization to new tasks [14, 22, 26, 27]. Using discrete skills as opposed to a goal-conditioned policy has also been explored in [13, 21]. All these approaches require the user to train a different skill for every automaton edge or a different goal-conditioned policy for every safety constraint that appears in the task, except for limited classes of safety constraints. This is impractical for most real-world tasks and, in particular, when safety constraints are changing throughout a task. Conversely, our method learns a single goal-conditioned policy for all goals in a particular LTL expression while still accounting for arbitrary, potentially non-stationary safety constraints. While ACQL has been developed for online RL rather than zero-shot generalization, there is a significant overlap in the tasks that both can ultimately solve. Therefore, we include the Logical Options Framework (LOF) [13] as a representative for these methods in our experiments.

Our work is also focused on solving LTL tasks that feature safety constraints. Safety constraints are often indirectly addressed in the methods discussed above. They primarily focus on making unsafe actions suboptimal by either terminating rollouts [8, 12, 36, 37] or applying negative reward shaping [13, 20, 32] when an unsafe automaton transition occurs. Other approaches based on formal methods, such as shielding [40, 41] and runtime model-checking [42], can more robustly enforce safety requirements but typically rely on additional assumptions such as access to a discrete abstraction of the environment or known system dynamics. In contrast, techniques from the Safe RL literature can still robustly enforce stationary safety constraints in complex environments without such assumptions [3, 4, 43–47]. Our approach builds on these Safe RL methods to address non-stationary safety constraints induced by LTL specifications.

3 Preliminaries

Constrained Reinforcement Learning RL problems with constraints are typically modeled as discounted CMDPs, which are defined by a tuple $(\mathcal{S}, \mathcal{A}, \mathcal{T}, d_0, r, c, \mathcal{L}, \gamma)$. This tuple consists of a state space $\mathcal{S}$, an action space $\mathcal{A}$, a transition function $\mathcal{T} : \mathcal{S} \times \mathcal{A} \to P(\mathcal{S})$ (where $P(\mathcal{S})$ represents the space of probability measures over $\mathcal{S}$), an initial state distribution $d_0 \in P(\mathcal{S})$, reward and constraint functions $r,\ c : \mathcal{S} \times \mathcal{A} \to \mathbb{R}$, a discount factor γ, and a limit for constraint violation $\mathcal{L} \in \mathbb{R}$ [3]. Given a CMDP, the standard objective is to find the stationary policy $\pi : \mathcal{S} \to P(\mathcal{A})$ satisfying the constrained maximization

$$\max_{\pi}\ J_r(\pi) \quad \text{s.t.} \quad J_c(\pi) < \mathcal{L}, \tag{1}$$

where $J_r(\pi) = \mathbb{E}_{\tau\sim\pi}\left[\sum_{t=0}^{\infty} \gamma^t r(s_t, a_t)\right]$ and $J_c(\pi) = \mathbb{E}_{\tau\sim\pi}\left[\sum_{t=0}^{\infty} \gamma^t c(s_t, a_t)\right]$ are respectively the expected total discounted return and cost of the policy π over trajectories $\tau = (s_0, a_0, s_1, a_1, \dots)$ induced by π through interactions with the environment of the CMDP. We denote the state value function of π by $V^r_\pi(s) = \mathbb{E}_\tau[\sum_{t=0}^{\infty} \gamma^t r(s_t, a_t)|s_0 = s]$ and the state-action value function by $Q^r_\pi(s, a) = \mathbb{E}_\tau[\sum_{t=0}^{\infty} \gamma^t r(s_t, a_t)|s_0 = s, a_0 = a]$.

Temporal Logic LTL [5] is an extension of propositional logic for reasoning about systems over time. LTL formulae $\phi \in \Phi$ consist of atomic propositions p from a set AP, the standard boolean operators "not" ($\neg$), "and" ($\wedge$), and "or" ($\vee$), and temporal operators that reference the value of propositions in the future. These operators are "next" ($\circ$), "eventually" ($\Diamond$), and "always" ($\Box$). We follow the definitions for these operators given in [48]. In our algorithm, we use Signal Temporal Logic (STL), which further extends LTL with quantitative semantics and requires that every atomic proposition $p \in AP$ is defined as a real-valued function of the system state. The quantitative semantics is defined by a function $\rho : \mathcal{S}^\omega \times \Phi \to \mathbb{R}$ that produces a robustness value representing how much a sequence of states $\omega \in \mathcal{S}^\omega$ satisfies or violates the property specified by an STL formula $\phi \in \Phi$. Our exact implementation of these quantitative semantics is based on [49]. Every temporal logic constraint can be expressed as the conjunction of a "safety" and "liveness" constraint [50], where a safety constraint is informally defined as a requirement that something must never happen for the task to succeed, and a liveness constraint is defined as a requirement that something must happen for the task to succeed. We take advantage of this dichotomy in our method.

Automata The robotics tasks discussed so far can be expressed more specifically as STL formulae in the recurrence class, as defined in [15], and all such formulae can be translated into abstract machines called Deterministic Büchi Automata (DBAs) [48]. A DBA is formally defined by the tuple $A = (\Sigma, \mathcal{Q}, \delta, q_0, F)$, consisting of an alphabet Σ, a set of internal states $\mathcal{Q}$, a transition function $\delta : \mathcal{Q} \times \Sigma \to \mathcal{Q}$, an initial state $q_0 \in \mathcal{Q}$, and a set of accepting states $F \subseteq \mathcal{Q}$. An automaton is used to process an infinite sequence of arbitrary symbols from the alphabet Σ and determine whether the sequence satisfies or does not satisfy the original logical expression. In our setting, a symbol processed by the automaton is a subset of atomic propositions $l \in 2^{AP}$ that are true in some MDP state $s \in \mathcal{S}$. This symbol l is referred to as the state's labeling and the mapping of states to their labeling is denoted by a labeling function $L : \mathcal{S} \to 2^{AP}$. The automaton A is always in some state $q \in \mathcal{Q}$, and starts in the state q_0. Each element $\sigma \in \Sigma$ of an input sequence causes some change in the automaton's internal state according to the transition function δ. For convenience, we will refer to edges in the automaton with transition predicates. A transition predicate is a propositional formula that holds for all $\sigma \in \Sigma$ which induce a transition between two states $q_i, q_j \in \mathcal{Q}$ according to δ [11]. By processing each state while an agent interacts with an MDP, the internal automaton state provides

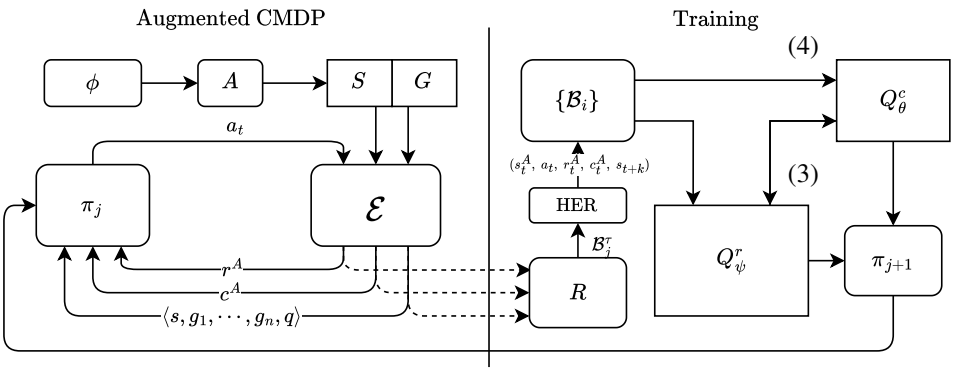

Figure 1: The ACQL algorithm relies on a novel augmented formulation of CMDPs (left). An input task specification ϕ is converted into the DBA A, from which safety constraints and subgoals are collected into mappings S and G respectively. The learning agent receives subgoals $g_1, \cdots, g_n$ at every stage in the task from G and safety constraint feedback in c^A from S. Trajectories induced by the policy π_j are collected into a replay buffer R, from which batches $\mathcal{B}^\tau_j$ are sampled and modified using HER [2]. From these modified trajectories, mini-batches $\mathcal{B}_i$ of transitions $(s^A_t, a_t, r^A_t, c^A_t, s^A_{t+1})$ are used to compute the targets y^r_t in (3) and y^c_t in (4) for training models of the state-action value function and safety function, Q^r_θ and Q^c_ψ, from which an updated policy π_{j+1} is derived.

information to the agent about its current progress in the task. This is the fundamental idea behind a Product MDP, which combines any MDP with a deterministic automaton and is a standard technique in model checking for probabilistic systems [48]. A complete definition for a product MDP in an RL context can be found in previous work such as [10, 37].

4 Method

This section introduces our ACQL algorithm along with a novel augmented product CMDP on which it is based. An overview is provided in Figure 1. First, we detail the construction of the augmented product CMDP derived from a task specification. Observations in this CMDP include the set of subgoals associated with the current automaton state q, as described in Section 3. This CMDP also uses safety conditions obtained from the task automaton to provide separate constraint feedback that the learning agent uses to determine safe actions. Unlike the standard CMDP constraint in (1), we argue for the use of a constraint on the minimum safety that is easier to learn. We finally present an overview and brief analysis of ACQL, which is tailored to utilize the information provided by our augmented product CMDP to scale beyond existing algorithms for learning in product MDPs.

4.1 Augmented Product CMDP Formulation

Obtaining the Automaton, Safety, and Liveness Constraints To construct the augmented product CMDP used by our algorithm, we begin by translating the input STL task specification ϕ into a DBA $A = (\Sigma, \mathcal{Q}, \delta, q_0, F)$ using the SPOT library [51]. As described in Section 3, this automaton represents the structure of the task. To better guide learning, we extract from this automaton additional structure that captures the task's safety and liveness requirements. Intuitively, these represent conditions that must *always* hold to avoid failure (safety) and conditions that must *eventually* hold to make progress toward task completion (liveness) [11, 50]. This information is summarized in two mappings: a safety condition mapping $S : \mathcal{Q} \to \Phi$, which assigns to each automaton state a proposition that must remain true, and a liveness condition mapping $O : \mathcal{Q} \to \Phi$, which assigns to each automaton state a proposition that must be eventually satisfied to proceed in the task. Based on O, we define $G : \mathcal{Q} \to \mathcal{G}^+$ to explicitly link automaton states to subgoals, where $\mathcal{G}^+ = \bigcup_{i=1}^{n} \mathcal{G}^i$ represents the full space of possible subgoal lists up to a task-dependent length n and $\mathcal{G}^i$ is the i-fold cartesian product of $\mathcal{G}$ with itself.

First, to obtain safety constraints, we determine the non-accepting sink-components of the automaton A; i.e., the automaton states $Q \setminus F$ from which there is no path to any state in F. For each automaton state q, we then examine the outgoing transitions from q that lead into these sink components. The predicates guarding these transitions describe conditions under which a transition into an unsafe state would occur, so negating these predicates provides the conditions that must hold in order to stay safe while in state q. We can then define $S(q)$ as the conjunction of all such negated predicates for state q.

Second, to obtain liveness constraints, we ignore the above transitions for safety conditions and examine the remaining predicates guarding outgoing transitions from each state q. These can only specify the conditions necessary to make progress in the task. Therefore, we can take the disjunction of these transition predicates to obtain the formula $O(q)$ that must be satisfied in order to transition beyond q. Following prior work on learning LTL tasks [13, 14], we assume that a subset of the atomic propositions, $AP_{\text{subgoal}} \subseteq AP$, represent subgoal propositions and are parameterized by values g within a subgoal space $\mathcal{G} \subseteq \mathcal{S}$. Note that we consider only a subset since not all the propositions in our modified DBA are necessarily related to achieving subgoals. Using this fact, we filter the predicates in $O(q)$ to retain only those associated with these subgoal propositions, which in turn provides a list of subgoals $G(q) = g_1, \ldots, g_n$ that are relevant to the logical formula given by $O(q)$. An illustrative example for these two steps is provided in the appendix.

Defining the Augmented Product CMDP Now, let $\mathcal{M}^A = (\mathcal{S}^A, \mathcal{A}^A, \mathcal{T}^A, d_0^A, r^A, c^A, \gamma, \mathcal{L})$ be a new CMDP formed by augmenting the original MDP $\mathcal{M} = (\mathcal{S}, \mathcal{A}, \mathcal{T}, d_0, r, \gamma)$ with the DBA $A = (\Sigma, \mathcal{Q}, \delta, q_0, F)$. The new state space $\mathcal{S}^A = \mathcal{S} \times \mathcal{G}^+ \times \mathcal{Q}$ is the Cartesian product of the original state space $\mathcal{S}$, the space for every possible list of subgoals $\mathcal{G}^+$, and the set of automaton states $\mathcal{Q}$. A state $s^A \in \mathcal{S}^A$ can be written as $\langle s, g^+, q \rangle$, where $s \in \mathcal{S}$, $g^+ \in \mathcal{G}^+$, and $q \in \mathcal{Q}$ are the constituent MDP state, goal-list and automaton state of s^A. The action space $\mathcal{A}^A = \mathcal{A}$ is unmodified. The new transition dynamics $\mathcal{T}^A$ are defined so that a transition to $\langle s', g^{+\prime}, q' \rangle \in \mathcal{S}^A$ from $\langle s, g^+, q \rangle \in \mathcal{S}^A$ is impossible if the automaton does not support a transition from q to q' when entering the state s'; i.e.,

$$\mathcal{T}^A(\langle s', g^{+\prime}, q' \rangle | \langle s, g^+, q \rangle, a) = \begin{cases} \mathcal{T}(s'|s, a) & \text{if } q' = \delta(q, L(s')), g^{+\prime} = G(q'), \\ 0 & \text{otherwise.} \end{cases}$$

Likewise, the initial state distribution $d_0^A(\langle s, g^+, q \rangle) = d_0(s)$ if $q = q_0$ and $g^+ = G(q_0)$, and is zero otherwise. The reward function $r^A(\langle s, g^+, q \rangle) = \mathbb{1}_F(q)$, where $\mathbb{1}(\cdot)$ is an indicator function, is defined to provide a sparse reward of 1 when the task is finished and the agent is near the goal associated with any accepting state of the automaton. Reward sparsity was a central shortcoming of prior work, often resulting in poor performance in realistic scenarios. However, our augmented product CMDP specifically includes the subgoal list g^+ to facilitate the use of modern GCRL algorithms to mitigate this sparsity in many relevant tasks. In particular, ACQL retroactively assigns rewards based on achieved subgoals using HER, and the benefit of this strategy for LTL-specified tasks is validated in our ablations (Section 5.3). Lastly, we define the constraint function c^A along with the constrained objective used with our CMDP formulation.

Minimum LTL Safety Constraint Although the sum-of-costs formulation in (1) conveniently leverages the standard Bellman equation, it presents practical challenges in learning. Specifically, predicting the cumulative sum of future costs requires accurately modeling long-term dependencies, which increases variance and slows down convergence. This can be appropriate for maximizing reward but unnecessarily complicated for safety. When dealing with safety. and in particular hard-safety [52], we are interesting in knowing whether the generated trajectory becomes unsafe at least once. Hence, this can be reformulated as a classification task. This approach bypasses the need for accurate regression by directly learning the decision boundary for state-action pairs leading to safety violations. To achieve this, we define a constraint function c^A such that it takes negative values if a safety constraint is violated and positive values otherwise, and we apply a constraint based on the minimum over all future values of $c^A(s_t^A, a_t)$. Then, we simply learn to classify this minimum value as being either positive or negative. This formulation allows us to determine safety violations in a single step, avoiding the complexity of cumulative cost prediction. A major advantage of this formulation is that it removes the need for manual tuning of the violation limit $\mathcal{L} \in \mathbb{R}$, which depends on the range of possible costs. Instead, by directly classifying actions as leading to a safety violation, we reduce the range of $\mathcal{L}$ to $[-1, 1]$. This normalization ensures robustness across tasks and allows for a simple, task-agnostic choice of $\mathcal{L} = 0$. Directly defining $c^A(\langle s, g^+, q \rangle, a) = \rho(s, S(q))$ using

Algorithm 1 Automaton Constrained Q-Learning

Require: An MDP $\mathcal{M} = (\mathcal{S}, \mathcal{A}, \mathcal{T}, d_0, r, \gamma)$, an STL specification $\phi \in \Phi$, a safety limit $\mathcal{L} \in [-1, 1]$, a learning rate α, an interpolation factor λ

1: $A \leftarrow \textsc{Translate}(\phi)$
2: $S, G \leftarrow \textsc{Partition}(A)$
3: $\mathcal{M}^A \leftarrow (\mathcal{S}^A, \mathcal{A}, \mathcal{T}^A, d_0^A, r^A, c^A, \gamma, L)$
4: $Q_\theta^c, Q_\psi^r \leftarrow \textsc{MakeNetworks}(\mathcal{S}^A, \mathcal{A})$
5: $\bar{\theta} \leftarrow \theta, \bar{\psi} \leftarrow \psi$
6: $R \leftarrow \textsc{MakeReplayBuffer}(\mathcal{M}^A)$
7: **for** $j = 1, \ldots, N$ **do**
8: $\quad \gamma_c \leftarrow \textsc{SafetyGammaScheduler}(j)$
9: $\quad \pi_j(s^A) \leftarrow \arg\max_{a : Q_\theta^c(s^A, a) > \mathcal{L}} Q_\psi^r(s^A, a)$
10: $\quad \tau \leftarrow \textsc{GetTrajectory}(\mathcal{M}^A, \pi_j)$
11: $\quad R \leftarrow R \cup \tau.$
12: $\quad \mathcal{B}_j^\tau \sim R$
13: $\quad \mathcal{B}_j^\tau \leftarrow \textsc{Relabel}(\mathcal{B}_j^\tau)$
14: $\quad$ **for** $i = 1, \ldots, M$ **do**
15: $\quad\quad \mathcal{B}_i \leftarrow \{(s_t^A, a_t, r_t, c_t, s_{t+1}^A)\} \sim \mathcal{B}_j^\tau$
16: $\quad\quad \theta \leftarrow \theta - \alpha \nabla_\theta L_{j,i}^c(\theta)$
17: $\quad\quad \psi \leftarrow \psi - \alpha \nabla_\psi L_{j,i}^r(\psi)$
18: $\quad\quad \bar{\theta} \leftarrow (1 - \lambda)\bar{\theta} + \lambda\theta, \bar{\psi} \leftarrow (1 - \lambda)\bar{\psi} + \lambda\psi$
19: $\quad$ **end for**
20: **end for**

the robustness function for $S(q)$ (see Section 3) satisfies this formulation and corresponds to the safety constraints for any STL-specified task.

Now, we can define our new objective as finding the optimal stationary policy $\pi^* : \mathcal{S} \to P(\mathcal{A})$ that maximizes the expected total discounted return, as defined in (1), while keeping the expected minimum safety above the safety limit $\mathcal{L}$:

$$\mathop{\mathbb{E}}_{\tau \sim \pi} \left[\min_{t \in [0, \infty]} c^A(s_t, a_t) \right] > \mathcal{L}, \tag{2}$$

where $\tau = (s_0^A, a_1, s_2^A, a_2, \ldots)$ is a trajectory within our augmented CMDP induced by the policy π. We denote this expected minimum safety for a policy π by its state-action safety function $Q_\pi^c(s, a) = \mathbb{E}_{\tau \sim \pi}[\min_{t=0}^\infty c^A(s_t^A, a_t) | s_0^A = s, a_0 = a]$.

4.2 Automaton Constrained Q-Learning (ACQL)

Overview In what follows, we provide an overview of the ACQL algorithm, whose pseudocode is shown in Algorithm 1. First, the input STL specification ϕ is translated into an automaton A (Line 1) that is partitioned to produce the mappings S and G (Line 2). These mappings and the automaton are combined with the input MDP $\mathcal{M}$ to create the augmented CMDP in Line 3. Using the augmented CMDP, ACQL can proceed to learn the optimal policy

$$\pi^*(s^A) = \mathop{\arg\max}_{a \,:\, Q^{c*}(s^A, a) > \mathcal{L}} Q^{r*}(s^A, a),$$

by learning the optimal state-action value function $Q^{r*} = Q_{\pi^*}^r$ and the optimal state-action safety function $Q^{c*} = Q_{\pi^*}^c$. In order to learn these optimal functions, we define the models $Q_\psi^r : \mathcal{S}^A \times \mathcal{A} \to \mathbb{R}$ and $Q_\theta^c : \mathcal{S}^A \times \mathcal{A} \to [-1, 1]$ parameterized by ψ and θ (Line 4). Their initial parameters are copied to initialize the target parameters $\bar{\theta}$ and $\bar{\psi}$ in Line 5, and an empty replay buffer is initialized in Line 6.

The algorithm proceeds to iterate for N epochs indexed by j. At each epoch, we obtain a value for the safety discount factor γ_c in Equation (4), which asymptotically approaches 1.0 as training progresses (Line 8). The policy π_j for the epoch is defined to select the most-rewarding action according to Q_ψ^r constrained by Q_θ^c (Line 9). A trajectory τ is collected according to an epsilon-greedy version of this

policy (Line 10), and this trajectory is added to the replay buffer (Line 11). From this replay buffer, a batch of trajectories $\mathcal{B}_j^\tau$ is sampled every epoch (Line 12). The inclusion of subgoals in the states s_t^A of the sampled mini-batch $\mathcal{B}_i$ allows us to further accelerate learning using relabeling techniques such as HER [2], which allows Q_θ^r to improve from failed attempts at progressing through the task. Mini-batches of transitions $\mathcal{B}_i$ are subsequently sampled from the relabeled trajectories (Line 15) and used to update Q_ψ^r for minimizing the loss

$$L_{j,i}^r(\psi) = \mathop{\mathbb{E}}_{(s_t^A, a_t)\sim\mathcal{B}_i}\left[\left(y_t^r - Q_\psi^r(s_t^A, a_t)\right)^2\right], \text{ with } y_t^r = r_t + \gamma Q_{\bar{\psi}}^r(s_{t+k}^A, \pi_j(s_{t+k}^A)). \tag{3}$$

Similarly, Q_θ^c is trained with the target

$$y_t^c = \gamma_c \min\{c^A(s_t^A, a_t),\ Q_{\bar{\theta}}^c(s_{t+1}^A, \pi_j(s_{t+1}^A))\} + (1-\gamma_c)\ c^A(s_t^A, a_t), \tag{4}$$

which is derived from the Bellman principle of optimality for expected minimum cost objectives given in [16]. The targets, y^r and y^c, are computed using target parameters, $\bar{\psi}$ and $\bar{\theta}$, which are updated towards their corresponding main parameters each step with an interpolation factor λ (Line 18). Crucially, we schedule the discount factor γ_c throughout training to asymptotically approach 1.0, which is necessary for convergence to Q^{c*}. Additional details for the subroutines used in Algorithm 1 are provided in the appendix.

Analysis Under mild assumptions, ACQL is guaranteed to asymptotically converge to the optimal solution. We summarize this in the following proposition:

Proposition 1. *Let $\mathcal{M}^\mathcal{A}$ be an augmented CMDP with $|\mathcal{S}^A| < \infty$, $|\mathcal{A}| < \infty$, and $\gamma \in [0, 1)$, and let Q_n^c and Q_n^r be models for the state-action safety and value functions indexed by n. Assume they are updated using Robbins-Monro step sizes $a(n)$ and $b(n)$, respectively, with $b(n) \in o(a(n))$ according to* (3) *and* (4)*. Assume that γ_{c_n} is also updated with step sizes $c(n)$ such that $\gamma_{c_n} \to 1$ and $c(n) \in o(b(n))$. Then Q_n^c and Q_n^r converge to Q^{c*} and Q^{r*} almost surely as $n \to \infty$.*

Proof Sketch. The step sizes $a(n)$, $b(n)$, and $c(n)$ create a stochastic approximation algorithm on three timescales [53]. Based on the contraction property of (4), the fastest updating Q_n^c asymptotically tracks the correct safety function for the policy determined by Q_n^r and γ_{c_n}. On the slower timescale ensured by the definition of $b(n)$ and $a(n)$, Q_n^r converges to the fixed point as determined by the relatively static γ_{c_n}, due to the contraction property of (3). Finally, as γ_c converges on the slowest timescale, the fixed points for the two faster timescales approach Q^{r*} and Q^{c*} at $\gamma_c = 1$. □

In Proposition 1, the notation $b(n) \in o(a(n))$ means that $b(n)/a(n) \to 0$ asymptotically. The assumption of a finite MDP is standard in the literature, but relaxing this assumption is possible by applying fixed point theorems for infinite dimensional spaces [54]. After convergence, the final policy will behave optimally for the reward r and (if possible) never incur any cost, thereby respecting the LTL safety constraint. A complete description of our algorithm, model implementation details, and a full proof of convergence, with reference to similar arguments used in prior work [43, 55, 56], are provided in the appendix.

5 Experiments

In this section, we justify the design of ACQL and evaluate its effectiveness. We conducted a comparative analysis of ACQL against established baselines in RL from LTL specifications, including RMs [12] and the LOF [13]. We demonstrate our method's real-world applicability by solving more complex LTL tasks with a 6-DOF robot arm in a storage cabinet environment. Lastly, we performed an ablation study to clarify how our subgoal-including product CMDP, in combination with HER [2], and our minimum-safety constraint formulation contribute to ACQL's performance.

5.1 Comparative Analysis

Baselines In selecting our baselines, we chose to not compare against standard Safe RL methods, offline policy learning methods, and multi-task LTL methods. Safe RL methods, without significant modification, cannot directly apply to LTL tasks and instead only address tasks with stationary safety constraints. Offline methods assume access to a fixed dataset and are not designed for the online

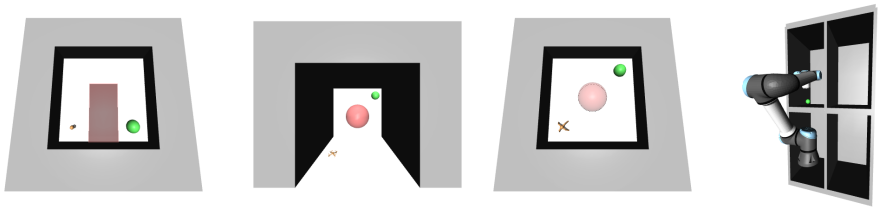

(a) PointMass Field (b) Quadcopter Room (c) Ant Field (d) UR5e Shelf

Figure 2: We conducted experiments in simulated environments for navigation tasks using a point mass, quadcopter, and ant quadruped. We also trained policies for end-effector control of a UR5e manipulator in a simulated shelf-environment for our real-world experiments.

Table 1: Results from policies trained for five task types in three different environments with 5 million environment interactions and 5 seeds. We report mean and one standard deviation of total reward and success rate in 16 evaluation episodes lasting 1000 steps over seeds for policies at the end of training.

		ACQL (Ours)		LOF [13]		CRM-RS [37]	
Robot	Task	Reward ↑	$S.R.(\%)$ ↑	Reward ↑	$S.R.(\%)$ ↑	Reward ↑	$S.R.(\%)$ ↑
P.M.	$\Diamond(g_1 \wedge \circ(\Diamond g_2))$	$\mathbf{829.6 \pm 9.6}$	$\mathbf{83.8 \pm 26.4}$	11.0 ± 3.1	98.8 ± 2.8	91.2 ± 4.3	0.0 ± 0.0
	$\Diamond g_1 \wedge \Diamond g_2$	$\mathbf{841.1 \pm 54.1}$	$\mathbf{98.8 \pm 2.8}$	470.7 ± 397.5	100.0 ± 0.0	420.6 ± 259.2	61.3 ± 38.6
	$\Diamond g_1 \wedge \Box\neg o_1$	$\mathbf{858.7 \pm 3.2}$	$\mathbf{100.0 \pm 0.0}$	0.0 ± 0.0	0.0 ± 0.0	0.0 ± 0.0	3.8 ± 8.4
	$\neg o_1 \mathcal{U} g_1 \wedge \circ\Diamond g_2$	$\mathbf{525.8 \pm 480.0}$	$\mathbf{60.0 \pm 54.8}$	0.0 ± 0.0	0.0 ± 0.0	0.0 ± 0.0	2.5 ± 5.6
	$\Box\Diamond(g_1 \wedge \circ\Diamond g_2) \wedge \Box\neg o_1$	$\mathbf{2.2 \pm 2.0}$	$\mathbf{62.5 \pm 41.8}$	0.0 ± 0.0	0.0 ± 0.0	0.0 ± 0.0	0.0 ± 0.0
Q.C.	$\Diamond(g_1 \wedge \circ(\Diamond g_2))$	$\mathbf{813.5 \pm 9.7}$	$\mathbf{100.0 \pm 0.0}$	32.0 ± 6.3	98.8 ± 2.8	0.0 ± 0.0	0.0 ± 0.0
	$\Diamond g_1 \wedge \Diamond g_2$	$\mathbf{752.6 \pm 157.0}$	$\mathbf{92.5 \pm 16.8}$	161.7 ± 287.6	92.5 ± 16.8	0.0 ± 0.0	0.0 ± 0.0
	$\Diamond g_1 \wedge \Box\neg o_1$	$\mathbf{822.7 \pm 107.4}$	$\mathbf{95.0 \pm 11.2}$	3.5 ± 5.9	15.0 ± 20.5	4.1 ± 9.2	2.5 ± 5.6
	$\neg o_1 \mathcal{U} g_1 \wedge \circ\Diamond g_2$	$\mathbf{726.6 \pm 88.6}$	$\mathbf{97.5 \pm 3.4}$	0.0 ± 0.0	0.0 ± 0.0	0.0 ± 0.0	0.0 ± 0.0
	$\Box\Diamond(g_1 \wedge \circ\Diamond g_2) \wedge \Box\neg o_1$	$\mathbf{2.4 \pm 1.2}$	$\mathbf{82.5 \pm 35.0}$	0.0 ± 0.0	0.0 ± 0.0	0.0 ± 0.0	0.0 ± 0.0
Ant	$\Diamond(g_1 \wedge \circ(\Diamond g_2))$	$\mathbf{555.8 \pm 39.8}$	$\mathbf{98.8 \pm 2.8}$	53.2 ± 29.8	91.2 ± 9.5	5.5 ± 12.3	1.2 ± 2.8
	$\Diamond g_1 \wedge \Diamond g_2$	$\mathbf{587.2 \pm 19.3}$	$\mathbf{98.8 \pm 2.8}$	158.0 ± 180.6	76.2 ± 42.7	4.6 ± 6.4	2.5 ± 3.4
	$\Diamond g_1 \wedge \Box\neg o_1$	$\mathbf{683.7 \pm 31.1}$	$\mathbf{85.0 \pm 3.4}$	38.3 ± 28.8	8.8 ± 7.1	0.0 ± 0.0	3.8 ± 3.4
	$\neg o_1 \mathcal{U} g_1 \wedge \circ\Diamond g_2$	$\mathbf{193.4 \pm 36.2}$	$\mathbf{87.5 \pm 10.8}$	0.0 ± 0.0	0.0 ± 0.0	0.0 ± 0.0	0.0 ± 0.0
	$\Box\Diamond(g_1 \wedge \circ\Diamond g_2) \wedge \Box\neg o_1$	$\mathbf{0.9 \pm 0.6}$	$\mathbf{77.5 \pm 12.9}$	0.0 ± 0.0	0.0 ± 0.0	0.0 ± 0.0	0.0 ± 0.0

learning setting we address. Multi-task methods [20, 22, 25, 27] take special measures to generalize across a distribution of LTL specifications. Comparisons to these methods in a single-task context would therefore require removing significant components from them and would not yield strong conclusions regarding their relative merit. We instead compared our algorithm against two methods for online RL with singular LTL specifications: Counterfactual Experiences for Reward Machines with Reward Shaping (CRM-RS) [37] and the LOF [13]. CRM-RS employs an RM to define the task and dispense shaped rewards that incentivize task completion. RM states in non-accepting sink components are treated as terminal states, implementing a rollout-terminating strategy to enforce safety constraints. The LOF is a framework for learning hierarchical policies to satisfy LTL tasks. It learns a separate policy, referred to as a logical option, for satisfying every subgoal-proposition in the task. When training each logical option, each step that violates the task's safety propositions receives a large reward penalty (set to $R_s = -1000$ based on their implementation) to discourage unsafe behavior. These policies are then composed with a higher-level policy obtained using value iteration over a discrete state space derived from the task automaton and all the subgoal states of the environment. Both these approaches can handle general LTL specifications and, to our knowledge, represent the most relevant baselines to compare our algorithm against. Furthermore, we note that RMs and the LOF cannot be easily enhanced with high-performing GCRL and Safe RL techniques without adopting substantial modifications to their learning algorithms and product MDP formulation. Our method effectively integrates these components in a single framework that enables learning from general logical objectives in complex settings, as demonstrated in the following tasks.

Tasks We chose five distinct LTL tasks and three different agents to facilitate a thorough comparison between our algorithm and the two baseline methods. All environment simulation was done within the Brax physics simulator [57]. The agents used in our experiments are a 2D PointMass, a Quadcopter, and an 8-DOF Ant quadruped. Additional details for these environments are given in the appendix. We used open environments without physical obstacles for our experiments. Instead, obstacles were introduced solely through the task specification. This was done to demonstrate the effectiveness of our algorithm in avoiding obstacles based purely on feedback from the task specifications, without

confounding effects such as physically restricted motion. The LTL tasks used in the evaluation include: (1) a two-subgoal sequential navigation task between opposite corners of the environment ($\Diamond(g_1 \wedge \circ(\Diamond g_2))$), (2) a two-subgoal branching navigation task between opposite corners of the environment ($\Diamond g_1 \wedge \Diamond g_2$), (3) a single-goal navigation task constrained by an unsafe region ($\Diamond g_1 \wedge \Box\neg o_1$), (4) a two-subgoal navigation task with a disappearing safety constraint ($\neg o_1 \mathcal{U} g_1 \wedge \circ\Diamond g_2$), and (5) an infinitely-looping navigation task with a persistent safety constraint ($\Box\Diamond(g_1 \wedge \circ\Diamond g_2) \wedge \Box\neg o_1$). The starting position, obstacle and subgoal configurations for each environment are shown in Figure 2.

Results The results for our three simulated environments and five task types are shown in Table 1. All results are reported for the final policy obtained after 5 million environment interactions with five different seeds. For LOF, each individual logical option was afforded its own 5 million training steps for fairness. For each seed, we evaluated the final policy in 16 randomly initialized episodes lasting 1000 steps. We report the reward, which corresponds to the number of steps spent near the final goal of the task automaton, and the success rate ($S.R.$), which is the proportion of policy rollouts that completely satisfied the task specification for all 1000 steps. Because the robustness of rollouts for the final "Loop" task cannot be meaningfully evaluated over a finite trajectory [58], we instead compute the success rate by examining the proportion of rollouts that are never unsafe and successfully complete at least 1 full loop within the episode.

We find that in these environments, stably reaching subgoals with any non-goal-conditioned method is unreliable, especially when rewards are delayed based on the task structure. As a result, CRM-RS fails for almost all environments and task types. The LOF is able to more easily scale to handle multiple goals due to its hierarchical structure and achieves high robustness for most rollouts. However, it also doesn't typically obtain high rewards due to only learning to apply options for reaching subgoals, as opposed to remaining near the final goal once the task is satisfied. Furthermore, the tasks with safety constraints clearly demonstrate that rollout termination in CRM-RS and the reward shaping used by LOF is insufficient for reliably preventing the agent from entering obstacle regions. Our method obtained significantly more reward than the baselines, while remaining consistently safe, in all five tasks and environments.

5.2 Real-World Experiments

As a first step in determining our algorithm's applicability to controlling robots in the real world for LTL specified tasks, we trained a policy using ACQL for controlling a 6-DOF manipulator in a storage cabinet workspace. We trained this policy in the simulated environment pictured in Figure 2d for a complex navigation task involving 3 subgoals and 2 obstacles: $\Diamond(p_1 \wedge \circ(\Diamond(p_2 \wedge \circ(\Diamond(p_3))))) \wedge \Box(\neg(\text{in\_wall} \vee \text{in\_table}))$. The policy was trained over 6 actions corresponding to translating the end-effector in the 6 cardinal directions. The geometry of the simulated environment perfectly aligned with the real cabinet workspace, so that policy actions based on the state of the simulation could be feasibly executed on the real robot. The resulting policy achieved a mean reward of 908.4 and a 100% success rate across 16 simulated rollouts, and we successfully deployed this same policy to the real UR5e robot arm and storage cabinet environment visualized in Figure 3. To support reproducibility, all relevant details for the task definition and environment setup are provided in our Supplementary Material. In future work, we intend to support a wider sim-to-real gap and train policies for LTL objectives in partially observable environments. Nonetheless, these initial results demonstrate that our algorithm can effectively leverage feedback from STL tasks in simulation to produce performant and safe policies for real robotic systems.

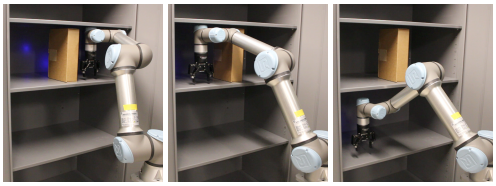

Figure 3: ACQL policies trained with safety constraints based a cabinet's geometry can be successfully deployed for a UR5e manipulator operating in the real cabinet environment.

5.3 Ablative Analysis

We conducted an additional ablative analysis to justify two key components of our algorithm. The results are reported in Table 2. In the first ablation, we removed the use of HER from ACQL, requiring the agent to learn exclusively from the sparse reward given upon reaching an accepting automaton

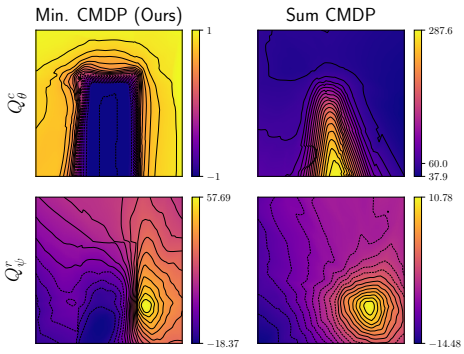

Figure 4: Contour plots for both Q^c_θ and Q^r_ψ trained with ACQL with our CMDP formulation in (2) and the standard formulation in (1).

Table 2: Results for our algorithm when ablating HER and substituting our minimum-safety CMDP formulation with the standard CMDP formulation. We report mean and standard deviation of the reward and success rate collected over all environments, tasks (except the loop task), and seeds from the policy at the end of training in 16 evaluation episodes lasting 1000 steps. For the ablation affecting safety constraints, we only report mean performance in tasks that include safety constraints.

		Reward ↑	$S.R.\%$ ↑
All Tasks	ACQL	$\mathbf{682.5 \pm 232.1}$	$\mathbf{91.5 \pm 20.3}$
	No HER	95.7 ± 220.1	12.9 ± 29.2
Safety Tasks	ACQL	$\mathbf{545.8 \pm 365.5}$	$\mathbf{75.4 \pm 39.1}$
	Sum CMDP	8.0 ± 24.9	4.6 ± 11.0

state. This ablation isolates the effect of our subgoal-including product CMDP formulation that enables applying GCRL methods in the context of LTL tasks, and our results show that removing it leads to significantly degraded performance.

Our second ablation demonstrates the benefit of our minimum safety constraint (2) over the discounted sum-of-cost framework (1) for accurately learning the state-action safety function. We modified our CMDP to provide positive costs when there was a safety violation, trained Q^c_θ to predict discounted sums of costs, and constrained π to choose actions below an upper limit on total cost $\mathcal{L}$. This limit was chosen based on the best performing value $\mathcal{L} \in \{0, 10, 40, 60\}$. We report the difference in performance over only the tasks that involved safety constraints and observe that our CMDP formulation is critical to the performance of our algorithm. We also show a visualization of the policy differences that result from this ablation in Figure 4. We observe that in our formulation (left), ACQL can more effectively learn the safety constraint, which substantially improves the quality of Q^r_ψ (bottom). Note that the differing scale for Q^c_θ in our formulation (top left) results in a yellow safe region, while the standard formulation depicts low-cost, safe regions in blue.

6 Conclusion

Limitations Although our method outperforms baseline methods in training policies to solve several fundamental types of LTL tasks, there remain a few limitations that we aim to address in future work. First, like many approaches leveraging product MDPs [13, 21, 32, 37], our method is restricted to logical tasks representable by DBAs. To overcome this, we plan to investigate more expressive types of automata for RL, such as Good-for-MDPs Non-Deterministic Büchi Automata [59]. Second, our current approach approximates the state-action value function without fully capturing task requirements beyond the current set of subgoals. We aim to explore more sophisticated goal-conditioned RL methods that can effectively condition a policy on future subgoals provided by our product CMDP. Finally, while our real-world deployment demonstrates the feasibility of applying our algorithm to robot control outside simulation, there are open challenges related to partial observability and sim-to-real mismatch in real-world learning with LTL objectives that we aim to address in future work.

We present a novel RL algorithm to tackle complex and high-dimensional LTL-specified tasks, enabled by a novel augmented product CMDP formulation that provides feedback for enforcing arbitrary safety constraints and subgoals for efficiently learning to achieve liveness constraints. By significantly outperforming comparable baselines for learning from LTL specifications, our approach demonstrates a promising trajectory toward learning in increasingly complex and realistic environments, without sacrificing generality in supporting the full expressiveness of LTL and other formal languages.

Acknowledgments

This material is based upon work supported by the Air Force Office of Scientific Research under award number FA9550-24-1-0233. Any opinions, findings, and conclusions or recommendations expressed in this material are those of the author(s) and do not necessarily reflect the views of the United States Air Force.

References

[1] Tom Schaul, Daniel Horgan, Karol Gregor, and David Silver. Universal value function approximators. In Francis Bach and David Blei, editors, *Proceedings of the 32nd International Conference on Machine Learning*, volume 37 of *Proceedings of Machine Learning Research*, pages 1312–1320, Lille, France, 07–09 Jul 2015. PMLR.

[2] Marcin Andrychowicz, Filip Wolski, Alex Ray, Jonas Schneider, Rachel Fong, Peter Welinder, Bob McGrew, Josh Tobin, OpenAI Pieter Abbeel, and Wojciech Zaremba. Hindsight experience replay. In I. Guyon, U. Von Luxburg, S. Bengio, H. Wallach, R. Fergus, S. Vishwanathan, and R. Garnett, editors, *Advances in Neural Information Processing Systems*, volume 30. Curran Associates, Inc., 2017.

[3] E. Altman. *Constrained Markov Decision Processes*. Stochastic Modeling Series. Taylor & Francis, 1999.

[4] Joshua Achiam, David Held, Aviv Tamar, and Pieter Abbeel. Constrained policy optimization. In Doina Precup and Yee Whye Teh, editors, *Proceedings of the 34th International Conference on Machine Learning*, volume 70 of *Proceedings of Machine Learning Research*, pages 22–31. PMLR, 06–11 Aug 2017.

[5] Amir Pnueli. The temporal logic of programs. In *18th Annual Symposium on Foundations of Computer Science (SFCS 1977)*, pages 46–57, 1977.

[6] Tuomas Haarnoja, Aurick Zhou, Pieter Abbeel, and Sergey Levine. Soft actor-critic: Off-policy maximum entropy deep reinforcement learning with a stochastic actor. *International Conference on Machine Learning (ICML)*, 2018.

[7] John Schulman, Filip Wolski, Prafulla Dhariwal, Alec Radford, and Oleg Klimov. Proximal policy optimization algorithms, 2017.

[8] Alberto Camacho, Rodrigo Toro Icarte, Toryn Q. Klassen, Richard Valenzano, and Sheila A. McIlraith. Ltl and beyond: Formal languages for reward function specification in reinforcement learning. In *Proceedings of the Twenty-Eighth International Joint Conference on Artificial Intelligence, IJCAI-19*, pages 6065–6073. International Joint Conferences on Artificial Intelligence Organization, July 2019.

[9] Mohammadhosein Hasanbeig, Alessandro Abate, and Daniel Kroening. Cautious reinforcement learning with logical constraints. In *Proceedings of the 19th International Conference on Autonomous Agents and MultiAgent Systems*, AAMAS '20, pages 483—491, Richland, SC, 2020. International Foundation for Autonomous Agents and Multiagent Systems.

[10] Mohammadhosein Hasanbeig, Daniel Kroening, and Alessandro Abate. Deep reinforcement learning with temporal logics. In Nathalie Bertrand and Nils Jansen, editors, *Formal Modeling and Analysis of Timed Systems*, pages 1–22, Cham, 2020. Springer International Publishing.

[11] Bowen Alpern and Fred B. Schneider. Recognizing safety and liveness. *Distributed Computing*, 2(3):117–126, September 1987.

[12] Rodrigo Toro Icarte, Toryn Klassen, Richard Valenzano, and Sheila McIlraith. Using reward machines for high-level task specification and decomposition in reinforcement learning. In Jennifer Dy and Andreas Krause, editors, *Proceedings of the 35th International Conference on Machine Learning*, volume 80 of *Proceedings of Machine Learning Research*, pages 2107–2116. PMLR, 10–15 Jul 2018.

[13] Brandon Araki, Xiao Li, Kiran Vodrahalli, Jonathan Decastro, Micah Fry, and Daniela Rus. The logical options framework. In Marina Meila and Tong Zhang, editors, *Proceedings of the 38th International Conference on Machine Learning*, volume 139 of *Proceedings of Machine Learning Research*, pages 307–317. PMLR, 18–24 Jul 2021.

[14] Wenjie Qiu, Wensen Mao, and He Zhu. Instructing goal-conditioned reinforcement learning agents with temporal logic objectives. In A. Oh, T. Naumann, A. Globerson, K. Saenko, M. Hardt, and S. Levine, editors, *Advances in Neural Information Processing Systems*, volume 36, pages 39147–39175. Curran Associates, Inc., 2023.

[15] Zohar Manna and Amir Pnueli. A hierarchy of temporal properties (invited paper, 1989). In *Proceedings of the Ninth Annual ACM Symposium on Principles of Distributed Computing*, PODC '90, pages 377—410, New York, NY, USA, 1990. Association for Computing Machinery.

[16] Jaime F. Fisac, Neil F. Lugovoy, Vicenç Rubies-Royo, Shromona Ghosh, and Claire J. Tomlin. Bridging hamilton-jacobi safety analysis and reinforcement learning. In *2019 International Conference on Robotics and Automation (ICRA)*, pages 8550–8556, 2019.

[17] Kai-Chieh Hsu, Vicenç Rubies-Royo, Claire J. Tomlin, and Jaime F. Fisac. Safety and liveness guarantees through reach-avoid reinforcement learning. In *Proceedings of Robotics: Science and Systems*, Held Virtually, July 2021.

[18] Xiao Li, Cristian-Ioan Vasile, and Calin Belta. Reinforcement learning with temporal logic rewards. In *2017 IEEE/RSJ International Conference on Intelligent Robots and Systems (IROS)*, pages 3834–3839, 2017.

[19] Xiao Li, Zachary Serlin, Guang Yang, and Calin Belta. A formal methods approach to interpretable reinforcement learning for robotic planning. *Science Robotics*, 4(37):eaay6276, 2019.

[20] Pashootan Vaezipoor, Andrew C Li, Rodrigo A Toro Icarte, and Sheila A. Mcilraith. LTL2Action: Generalizing LTL instructions for multi-task RL. In Marina Meila and Tong Zhang, editors, *Proceedings of the 38th International Conference on Machine Learning*, volume 139 of *Proceedings of Machine Learning Research*, pages 10497–10508. PMLR, 18–24 Jul 2021.

[21] Geraud Nangue Tasse, Steven James, and Benjamin Rosman. Skill machines: Temporal logic composition in reinforcement learning. In *Deep Reinforcement Learning Workshop @ NeurIPS*, 2022.

[22] Beyazit Yalcinkaya, Niklas Lauffer, Marcell Vazquez-Chanlatte, and Sanjit Seshia. Automata conditioned reinforcement learning with experience replay. In *NeurIPS 2023 Workshop on Goal-Conditioned Reinforcement Learning*, 2023.

[23] Zikang Xiong, Daniel Lawson, Joe Eappen, Ahmed H. Qureshi, and Suresh Jagannathan. Co-learning planning and control policies constrained by differentiable logic specifications. In *2024 IEEE International Conference on Robotics and Automation (ICRA)*, pages 14272–14278, 2024.

[24] Duo Xu and Faramarz Fekri. Generalization of temporal logic tasks via future dependent options. *Machine Learning*, 113(10):7509–7540, October 2024.

[25] Beyazit Yalcinkaya, Niklas Lauffer, Marcell Vazquez-Chanlatte, and Sanjit A. Seshia. Compositional automata embeddings for goal-conditioned reinforcement learning. In A. Globerson, L. Mackey, D. Belgrave, A. Fan, U. Paquet, J. Tomczak, and C. Zhang, editors, *Advances in Neural Information Processing Systems*, volume 37, pages 72933–72963. Curran Associates, Inc., 2024.

[26] Beyazit Yalcinkaya, Niklas Lauffer, Marcell Vazquez-Chanlatte, and Sanjit A. Seshia. Provably correct automata embeddings for optimal automata-conditioned reinforcement learning. In George Pappas, Pradeep Ravikumar, and Sanjit A. Seshia, editors, *Proceedings of the International Conference on Neuro-symbolic Systems*, volume 288 of *Proceedings of Machine Learning Research*, pages 661–675. PMLR, 28–30 May 2025.

[27] Mathias Jackermeier and Alessandro Abate. DeepLTL: Learning to efficiently satisfy complex LTL specifications for multi-task RL. In *The Thirteenth International Conference on Learning Representations*, 2025.

[28] Ameesh Shah, Cameron Voloshin, Chenxi Yang, Abhinav Verma, Swarat Chaudhuri, and Sanjit A. Seshia. LTL-constrained policy optimization with cycle experience replay. *Transactions on Machine Learning Research*, 2025.

[29] Xiao Li, Yao Ma, and Calin Belta. A policy search method for temporal logic specified reinforcement learning tasks. In *2018 Annual American Control Conference (ACC)*, pages 240–245, 2018.

[30] Derya Aksaray, Austin Jones, Zhaodan Kong, Mac Schwager, and Calin Belta. Q-learning for robust satisfaction of signal temporal logic specifications. In *2016 IEEE 55th Conference on Decision and Control (CDC)*, pages 6565–6570, 2016.

[31] Anand Balakrishnan and Jyotirmoy V. Deshmukh. Structured reward shaping using signal temporal logic specifications. In *2019 IEEE/RSJ International Conference on Intelligent Robots and Systems (IROS)*, pages 3481–3486, 2019.

[32] Eleanor Quint, Dong Xu, Samuel W Flint, Stephen D Scott, and Matthew Dwyer. Formal language constrained markov decision processes, 2021.

[33] Xiao Li, Yao Ma, and Calin Belta. Automata-guided hierarchical reinforcement learning for skill composition, 2018.

[34] Geraud Nangue Tasse, Steven James, and Benjamin Rosman. A boolean task algebra for reinforcement learning. In H. Larochelle, M. Ranzato, R. Hadsell, M.F. Balcan, and H. Lin, editors, *Advances in Neural Information Processing Systems*, volume 33, pages 9497–9507. Curran Associates, Inc., 2020.

[35] Kishor Jothimurugan, Suguman Bansal, Osbert Bastani, and Rajeev Alur. Compositional reinforcement learning from logical specifications. *Advances in Neural Information Processing Systems*, 34:10026–10039, 2021.

[36] Mohammadhosein Hasanbeig, Alessandro Abate, and Daniel Kroening. Logically-constrained reinforcement learning, 2019.

[37] Rodrigo Toro Icarte, Toryn Q. Klassen, Richard Valenzano, and Sheila A. McIlraith. Reward machines: Exploiting reward function structure in reinforcement learning. *Journal of Artificial Intelligence Research*, 73:173—208, January 2022.

[38] Leslie Pack Kaelbling. Learning to achieve goals. In *International Joint Conference on Artificial Intelligence*, volume 2, pages 1094–8. Citeseer, 1993.

[39] Tom Schaul, Daniel Horgan, Karol Gregor, and David Silver. Universal value function approximators. In *International Conference on Machine Learning*, pages 1312–1320. PMLR, 2015.

[40] Mohammed Alshiekh, Roderick Bloem, Rüdiger Ehlers, Bettina Könighofer, Scott Niekum, and Ufuk Topcu. Safe reinforcement learning via shielding. *Proceedings of the AAAI Conference on Artificial Intelligence*, 32(1), April 2018.

[41] Bettina Könighofer, Julian Rudolf, Alexander Palmisano, Martin Tappler, and Roderick Bloem. Online shielding for reinforcement learning. *Innovations in Systems and Software Engineering*, 19(4):379–394, December 2023.

[42] Ankush Desai, Tommaso Dreossi, and Sanjit A. Seshia. Combining model checking and runtime verification for safe robotics. In Shuvendu Lahiri and Giles Reger, editors, *Runtime Verification*, pages 172–189, Cham, 2017. Springer International Publishing.

[43] Dongjie Yu, Haitong Ma, Shengbo Li, and Jianyu Chen. Reachability constrained reinforcement learning. In Kamalika Chaudhuri, Stefanie Jegelka, Le Song, Csaba Szepesvari, Gang Niu, and Sivan Sabato, editors, *Proceedings of the 39th International Conference on Machine Learning*, volume 162 of *Proceedings of Machine Learning Research*, pages 25636–25655. PMLR, 17–23 Jul 2022.

[44] Gabriel Kalweit, Maria Huegle, Moritz Werling, and Joschka Boedecker. Deep constrained Q-learning, 2020.

[45] Adam Stooke, Joshua Achiam, and Pieter Abbeel. Responsive safety in reinforcement learning by pid lagrangian methods. In *Proceedings of the 37th International Conference on Machine Learning*, ICML'20. JMLR.org, 2020.

[46] Sehoon Ha, Peng Xu, Zhenyu Tan, Sergey Levine, and Jie Tan. Learning to walk in the real world with minimal human effort. In Jens Kober, Fabio Ramos, and Claire Tomlin, editors, *Proceedings of the 2020 Conference on Robot Learning*, volume 155 of *Proceedings of Machine Learning Research*, pages 1110–1120. PMLR, 16–18 Nov 2021.

[47] Yongshuai Liu, Jiaxin Ding, and Xin Liu. Ipo: Interior-point policy optimization under constraints. *Proceedings of the AAAI Conference on Artificial Intelligence*, 34(04):4940–4947, April 2020.

[48] C. Baier, J.P. Katoen, and K.G. Larsen. *Principles of Model Checking*. MIT Press, 2008.

[49] Charles Dawson and Chuchu Fan. Robust counterexample-guided optimization for planning from differentiable temporal logic. In *2022 IEEE/RSJ International Conference on Intelligent Robots and Systems (IROS)*, pages 7205–7212, 2022.

[50] Bowen Alpern and Fred Schneider. Defining liveness. *Information Processing Letters*, 21(4):181–185, 1985.

[51] Alexandre Duret-Lutz, Etienne Renault, Maximilien Colange, Florian Renkin, Alexandre Gbaguidi Aisse, Philipp Schlehuber-Caissier, Thomas Medioni, Antoine Martin, Jérôme Dubois, Clément Gillard, and Henrich Lauko. From Spot 2.0 to Spot 2.10: What's new? In *Proceedings of the 34th International Conference on Computer Aided Verification (CAV'22)*, volume 13372 of *Lecture Notes in Computer Science*, pages 174–187. Springer, August 2022.

[52] Yixuan Wang, Simon Sinong Zhan, Ruochen Jiao, Zhilu Wang, Wanxin Jin, Zhuoran Yang, Zhaoran Wang, Chao Huang, and Qi Zhu. Enforcing hard constraints with soft barriers: safe reinforcement learning in unknown stochastic environments. In *Proceedings of the 40th International Conference on Machine Learning*, ICML'23. JMLR.org, 2023.

[53] Vivek S. Borkar. *Stochastic Approximation: A Dynamical Systems Viewpoint*. Hindustan Book Agency Gurgaon, 2008.

[54] A. Granas and J. Dugundji. *Fixed Point Theory*. Monographs in Mathematics. Springer, 2003.

[55] Haitong Ma, Changliu Liu, Shengbo Eben Li, Sifa Zheng, and Jianyu Chen. Joint synthesis of safety certificate and safe control policy using constrained reinforcement learning. In Roya Firoozi, Negar Mehr, Esen Yel, Rika Antonova, Jeannette Bohg, Mac Schwager, and Mykel Kochenderfer, editors, *Proceedings of The 4th Annual Learning for Dynamics and Control Conference*, volume 168 of *Proceedings of Machine Learning Research*, pages 97–109. PMLR, 23–24 Jun 2022.

[56] Yinlam Chow, Mohammad Ghavamzadeh, Lucas Janson, and Marco Pavone. Risk-constrained reinforcement learning with percentile risk criteria, 2017.

[57] C. Daniel Freeman, Erik Frey, Anton Raichuk, Sertan Girgin, Igor Mordatch, and Olivier Bachem. Brax - a differentiable physics engine for large scale rigid body simulation, 2021.

[58] Ernst Moritz Hahn, Mateo Perez, Sven Schewe, Fabio Somenzi, Ashutosh Trivedi, and Dominik Wojtczak. Omega-regular objectives in model-free reinforcement learning. In Tomáš Vojnar and Lijun Zhang, editors, *Tools and Algorithms for the Construction and Analysis of Systems*, pages 395–412, Cham, 2019. Springer International Publishing.

[59] Ernst Moritz Hahn, Mateo Perez, Sven Schewe, Fabio Somenzi, Ashutosh Trivedi, and Dominik Wojtczak. Good-for-mdps automata for probabilistic analysis and reinforcement learning. In Armin Biere and David Parker, editors, *Tools and Algorithms for the Construction and Analysis of Systems*, pages 306–323, Cham, 2020. Springer International Publishing.

[60] John N. Tsitsiklis. Asynchronous stochastic approximation and Q-learning. *Machine Learning*, 16(3):185–202, September 1994.

[61] D. Bertsekas and J. Tsitsiklis. *Parallel and Distributed Computation: Numerical Methods*. Athena Scientific, 2015.

[62] Michał Bortkiewicz, Władek Pałucki, Vivek Myers, Tadeusz Dziarmaga, Tomasz Arczewski, Łukasz Kuciński, and Benjamin Eysenbach. Accelerating goal-conditioned RL algorithms and research. *arXiv preprint arXiv: 2408.11052*, 2024.

NeurIPS Paper Checklist

1. **Claims**

   Question: Do the main claims made in the abstract and introduction accurately reflect the paper's contributions and scope?

   Answer: [Yes]

   Justification: The abstract and introduction clearly state that we contribute a novel algorithm for learning tasks specified with LTL formulae (in the recurrence class) that scales to high-dimensional environments better than similarly general existing algorithms. Our experimental results support this claim.

   Guidelines:

   - The answer NA means that the abstract and introduction do not include the claims made in the paper.
   - The abstract and/or introduction should clearly state the claims made, including the contributions made in the paper and important assumptions and limitations. A No or NA answer to this question will not be perceived well by the reviewers.
   - The claims made should match theoretical and experimental results, and reflect how much the results can be expected to generalize to other settings.
   - It is fine to include aspirational goals as motivation as long as it is clear that these goals are not attained by the paper.

2. **Limitations**

   Question: Does the paper discuss the limitations of the work performed by the authors?

   Answer: [Yes]

   Justification: In Paragraph 6, we clearly describe that our algorithm is limited to STL formulae in the recurrence class (representable as DBAs). We also describe in the paper that these formulae are defined over a set of atomic propositions with non-safety-related propositions being tied to specific goals in a goal space $\mathcal{G} \subseteq \mathcal{S}$. We also state that our policy is only conditioned on the current set of subgoals, and therefore limited to optimal decision-making only for those subgoals without accounting for future subgoal requirements.

   Guidelines:

   - The answer NA means that the paper has no limitation while the answer No means that the paper has limitations, but those are not discussed in the paper.
   - The authors are encouraged to create a separate "Limitations" section in their paper.
   - The paper should point out any strong assumptions and how robust the results are to violations of these assumptions (e.g., independence assumptions, noiseless settings, model well-specification, asymptotic approximations only holding locally). The authors should reflect on how these assumptions might be violated in practice and what the implications would be.

- The authors should reflect on the scope of the claims made, e.g., if the approach was only tested on a few datasets or with a few runs. In general, empirical results often depend on implicit assumptions, which should be articulated.
- The authors should reflect on the factors that influence the performance of the approach. For example, a facial recognition algorithm may perform poorly when image resolution is low or images are taken in low lighting. Or a speech-to-text system might not be used reliably to provide closed captions for online lectures because it fails to handle technical jargon.
- The authors should discuss the computational efficiency of the proposed algorithms and how they scale with dataset size.
- If applicable, the authors should discuss possible limitations of their approach to address problems of privacy and fairness.
- While the authors might fear that complete honesty about limitations might be used by reviewers as grounds for rejection, a worse outcome might be that reviewers discover limitations that aren't acknowledged in the paper. The authors should use their best judgment and recognize that individual actions in favor of transparency play an important role in developing norms that preserve the integrity of the community. Reviewers will be specifically instructed to not penalize honesty concerning limitations.

3. **Theory assumptions and proofs**

   Question: For each theoretical result, does the paper provide the full set of assumptions and a complete (and correct) proof?

   Answer: [Yes]

   Justification: All assumptions are provided for our one (informal) theoretical claim in Section 4.2, and a complete and correct proof is included in the appendix.

   Guidelines:

   - The answer NA means that the paper does not include theoretical results.
   - All the theorems, formulas, and proofs in the paper should be numbered and cross-referenced.
   - All assumptions should be clearly stated or referenced in the statement of any theorems.
   - The proofs can either appear in the main paper or the supplemental material, but if they appear in the supplemental material, the authors are encouraged to provide a short proof sketch to provide intuition.
   - Inversely, any informal proof provided in the core of the paper should be complemented by formal proofs provided in appendix or supplemental material.
   - Theorems and Lemmas that the proof relies upon should be properly referenced.

4. **Experimental result reproducibility**

   Question: Does the paper fully disclose all the information needed to reproduce the main experimental results of the paper to the extent that it affects the main claims and/or conclusions of the paper (regardless of whether the code and data are provided or not)?

   Answer: [Yes]

   Justification: Algorithm and environment implementation details, including relevant hyper parameters, are disclosed in the paper to an extent that should allow reproduction of the experiments. Additional resources to facilitate reproducibility are provided in code which is included as a link in the paper.

   Guidelines:

   - The answer NA means that the paper does not include experiments.
   - If the paper includes experiments, a No answer to this question will not be perceived well by the reviewers: Making the paper reproducible is important, regardless of whether the code and data are provided or not.
   - If the contribution is a dataset and/or model, the authors should describe the steps taken to make their results reproducible or verifiable.

- Depending on the contribution, reproducibility can be accomplished in various ways. For example, if the contribution is a novel architecture, describing the architecture fully might suffice, or if the contribution is a specific model and empirical evaluation, it may be necessary to either make it possible for others to replicate the model with the same dataset, or provide access to the model. In general. releasing code and data is often one good way to accomplish this, but reproducibility can also be provided via detailed instructions for how to replicate the results, access to a hosted model (e.g., in the case of a large language model), releasing of a model checkpoint, or other means that are appropriate to the research performed.
- While NeurIPS does not require releasing code, the conference does require all submissions to provide some reasonable avenue for reproducibility, which may depend on the nature of the contribution. For example
  (a) If the contribution is primarily a new algorithm, the paper should make it clear how to reproduce that algorithm.
  (b) If the contribution is primarily a new model architecture, the paper should describe the architecture clearly and fully.
  (c) If the contribution is a new model (e.g., a large language model), then there should either be a way to access this model for reproducing the results or a way to reproduce the model (e.g., with an open-source dataset or instructions for how to construct the dataset).
  (d) We recognize that reproducibility may be tricky in some cases, in which case authors are welcome to describe the particular way they provide for reproducibility. In the case of closed-source models, it may be that access to the model is limited in some way (e.g., to registered users), but it should be possible for other researchers to have some path to reproducing or verifying the results.

5. **Open access to data and code**

   Question: Does the paper provide open access to the data and code, with sufficient instructions to faithfully reproduce the main experimental results, as described in supplemental material?

   Answer: [Yes]

   Justification: We provide open access to anonymized code, along with scripts and an exact description of all required dependencies with version information, needed for running all of our experiments.

   Guidelines:

   - The answer NA means that paper does not include experiments requiring code.
   - Please see the NeurIPS code and data submission guidelines (`https://nips.cc/public/guides/CodeSubmissionPolicy`) for more details.
   - While we encourage the release of code and data, we understand that this might not be possible, so "No" is an acceptable answer. Papers cannot be rejected simply for not including code, unless this is central to the contribution (e.g., for a new open-source benchmark).
   - The instructions should contain the exact command and environment needed to run to reproduce the results. See the NeurIPS code and data submission guidelines (`https://nips.cc/public/guides/CodeSubmissionPolicy`) for more details.
   - The authors should provide instructions on data access and preparation, including how to access the raw data, preprocessed data, intermediate data, and generated data, etc.
   - The authors should provide scripts to reproduce all experimental results for the new proposed method and baselines. If only a subset of experiments are reproducible, they should state which ones are omitted from the script and why.
   - At submission time, to preserve anonymity, the authors should release anonymized versions (if applicable).
   - Providing as much information as possible in supplemental material (appended to the paper) is recommended, but including URLs to data and code is permitted.

6. **Experimental setting/details**

Question: Does the paper specify all the training and test details (e.g., data splits, hyperparameters, how they were chosen, type of optimizer, etc.) necessary to understand the results?

Answer: [Yes]

Justification: All training and test information is included in the paper to understand the results, and additional information is included in our supplementary material.

Guidelines:

- The answer NA means that the paper does not include experiments.
- The experimental setting should be presented in the core of the paper to a level of detail that is necessary to appreciate the results and make sense of them.
- The full details can be provided either with the code, in appendix, or as supplemental material.

7. **Experiment statistical significance**

Question: Does the paper report error bars suitably and correctly defined or other appropriate information about the statistical significance of the experiments?

Answer: [Yes]

Justification: In Sections 5.1 and 5.3, we report the variance across trials using one standard deviation.

Guidelines:

- The answer NA means that the paper does not include experiments.
- The authors should answer "Yes" if the results are accompanied by error bars, confidence intervals, or statistical significance tests, at least for the experiments that support the main claims of the paper.
- The factors of variability that the error bars are capturing should be clearly stated (for example, train/test split, initialization, random drawing of some parameter, or overall run with given experimental conditions).
- The method for calculating the error bars should be explained (closed form formula, call to a library function, bootstrap, etc.)
- The assumptions made should be given (e.g., Normally distributed errors).
- It should be clear whether the error bar is the standard deviation or the standard error of the mean.
- It is OK to report 1-sigma error bars, but one should state it. The authors should preferably report a 2-sigma error bar than state that they have a 96% CI, if the hypothesis of Normality of errors is not verified.
- For asymmetric distributions, the authors should be careful not to show in tables or figures symmetric error bars that would yield results that are out of range (e.g. negative error rates).
- If error bars are reported in tables or plots, The authors should explain in the text how they were calculated and reference the corresponding figures or tables in the text.

8. **Experiments compute resources**

Question: For each experiment, does the paper provide sufficient information on the computer resources (type of compute workers, memory, time of execution) needed to reproduce the experiments?

Answer: [Yes]

Justification: In the appendix, we report the total computer resources needed for our experiments.

Guidelines:

- The answer NA means that the paper does not include experiments.
- The paper should indicate the type of compute workers CPU or GPU, internal cluster, or cloud provider, including relevant memory and storage.
- The paper should provide the amount of compute required for each of the individual experimental runs as well as estimate the total compute.

- The paper should disclose whether the full research project required more compute than the experiments reported in the paper (e.g., preliminary or failed experiments that didn't make it into the paper).

9. **Code of ethics**

   Question: Does the research conducted in the paper conform, in every respect, with the NeurIPS Code of Ethics `https://neurips.cc/public/EthicsGuidelines`?

   Answer: [Yes]

   Justification: This research (1) does not involve human subjects or participants, (2) does not involve any datasets, (3) has negligible foreseeable societal impact with regard to human safety, security, discrimination, surveillance, deception, harassment, the environment, or human rights issues, (4) does not contain or exacerbate biases against groups of people, and (5) includes in its supplementary material a correctly documented, licensed, and anonymized code base that is sufficient for reproducing the results.

   Guidelines:

   - The answer NA means that the authors have not reviewed the NeurIPS Code of Ethics.
   - If the authors answer No, they should explain the special circumstances that require a deviation from the Code of Ethics.
   - The authors should make sure to preserve anonymity (e.g., if there is a special consideration due to laws or regulations in their jurisdiction).

10. **Broader impacts**

    Question: Does the paper discuss both potential positive societal impacts and negative societal impacts of the work performed?

    Answer: [Yes]

    Justification: We include a discussion of the foreseeable societal consequences of this work in our appendix.

    Guidelines:

    - The answer NA means that there is no societal impact of the work performed.
    - If the authors answer NA or No, they should explain why their work has no societal impact or why the paper does not address societal impact.
    - Examples of negative societal impacts include potential malicious or unintended uses (e.g., disinformation, generating fake profiles, surveillance), fairness considerations (e.g., deployment of technologies that could make decisions that unfairly impact specific groups), privacy considerations, and security considerations.
    - The conference expects that many papers will be foundational research and not tied to particular applications, let alone deployments. However, if there is a direct path to any negative applications, the authors should point it out. For example, it is legitimate to point out that an improvement in the quality of generative models could be used to generate deepfakes for disinformation. On the other hand, it is not needed to point out that a generic algorithm for optimizing neural networks could enable people to train models that generate Deepfakes faster.
    - The authors should consider possible harms that could arise when the technology is being used as intended and functioning correctly, harms that could arise when the technology is being used as intended but gives incorrect results, and harms following from (intentional or unintentional) misuse of the technology.
    - If there are negative societal impacts, the authors could also discuss possible mitigation strategies (e.g., gated release of models, providing defenses in addition to attacks, mechanisms for monitoring misuse, mechanisms to monitor how a system learns from feedback over time, improving the efficiency and accessibility of ML).

11. **Safeguards**

    Question: Does the paper describe safeguards that have been put in place for responsible release of data or models that have a high risk for misuse (e.g., pretrained language models, image generators, or scraped datasets)?

    Answer: [NA]

Justification: This work has not produced artifacts that pose such risks.

Guidelines:

- The answer NA means that the paper poses no such risks.
- Released models that have a high risk for misuse or dual-use should be released with necessary safeguards to allow for controlled use of the model, for example by requiring that users adhere to usage guidelines or restrictions to access the model or implementing safety filters.
- Datasets that have been scraped from the Internet could pose safety risks. The authors should describe how they avoided releasing unsafe images.
- We recognize that providing effective safeguards is challenging, and many papers do not require this, but we encourage authors to take this into account and make a best faith effort.

12. **Licenses for existing assets**

Question: Are the creators or original owners of assets (e.g., code, data, models), used in the paper, properly credited and are the license and terms of use explicitly mentioned and properly respected?

Answer: [Yes]

Justification: Our code uses the following libraries: (1) Brax (Apache License 2.0), (2) Mujoco Menagerie (MIT), (3) JaxGCRL (Apache 2.0), (4) Spot (GPLv3). Our paper cites these when discussing implementation details in the appendix. Our code abides by these and other licenses and is itself licensed with the GPLv3 license.

Guidelines:

- The answer NA means that the paper does not use existing assets.
- The authors should cite the original paper that produced the code package or dataset.
- The authors should state which version of the asset is used and, if possible, include a URL.
- The name of the license (e.g., CC-BY 4.0) should be included for each asset.
- For scraped data from a particular source (e.g., website), the copyright and terms of service of that source should be provided.
- If assets are released, the license, copyright information, and terms of use in the package should be provided. For popular datasets, `paperswithcode.com/datasets` has curated licenses for some datasets. Their licensing guide can help determine the license of a dataset.
- For existing datasets that are re-packaged, both the original license and the license of the derived asset (if it has changed) should be provided.
- If this information is not available online, the authors are encouraged to reach out to the asset's creators.

13. **New assets**

Question: Are new assets introduced in the paper well documented and is the documentation provided alongside the assets?

Answer: [Yes]

Justification: We include our anonymized code base as one asset and provide alongside it the necessary documentation.

Guidelines:

- The answer NA means that the paper does not release new assets.
- Researchers should communicate the details of the dataset/code/model as part of their submissions via structured templates. This includes details about training, license, limitations, etc.
- The paper should discuss whether and how consent was obtained from people whose asset is used.
- At submission time, remember to anonymize your assets (if applicable). You can either create an anonymized URL or include an anonymized zip file.

14. **Crowdsourcing and research with human subjects**

    Question: For crowdsourcing experiments and research with human subjects, does the paper include the full text of instructions given to participants and screenshots, if applicable, as well as details about compensation (if any)?

    Answer: [NA]

    Justification: This research did not involve crowdsourcing nor research with human subjects.

    Guidelines:

    - The answer NA means that the paper does not involve crowdsourcing nor research with human subjects.
    - Including this information in the supplemental material is fine, but if the main contribution of the paper involves human subjects, then as much detail as possible should be included in the main paper.
    - According to the NeurIPS Code of Ethics, workers involved in data collection, curation, or other labor should be paid at least the minimum wage in the country of the data collector.

15. **Institutional review board (IRB) approvals or equivalent for research with human subjects**

    Question: Does the paper describe potential risks incurred by study participants, whether such risks were disclosed to the subjects, and whether Institutional Review Board (IRB) approvals (or an equivalent approval/review based on the requirements of your country or institution) were obtained?

    Answer: [NA]

    Justification: This research did not involve crowdsourcing nor research with human subjects.

    Guidelines:

    - The answer NA means that the paper does not involve crowdsourcing nor research with human subjects.
    - Depending on the country in which research is conducted, IRB approval (or equivalent) may be required for any human subjects research. If you obtained IRB approval, you should clearly state this in the paper.
    - We recognize that the procedures for this may vary significantly between institutions and locations, and we expect authors to adhere to the NeurIPS Code of Ethics and the guidelines for their institution.
    - For initial submissions, do not include any information that would break anonymity (if applicable), such as the institution conducting the review.

16. **Declaration of LLM usage**

    Question: Does the paper describe the usage of LLMs if it is an important, original, or non-standard component of the core methods in this research? Note that if the LLM is used only for writing, editing, or formatting purposes and does not impact the core methodology, scientific rigorousness, or originality of the research, declaration is not required.

    Answer: [NA]

    Justification: The method developed in this research does not involve LLMs.

    Guidelines:

    - The answer NA means that the core method development in this research does not involve LLMs as any important, original, or non-standard components.
    - Please refer to our LLM policy (`https://neurips.cc/Conferences/2025/LLM`) for what should or should not be described.

A Proof of Proposition 1

In what follows, we formally prove and restate Proposition 1, which shows that ACQL, under mild conditions, is guaranteed to return the optimal policy. Our proof is based on the proof of convergence for Q-learning using stochastic approximation theory in [60], extended with the theory of stochastic approximation under multiple timescales described in Chapter 6 of [53]. Refer also to [43, 55, 56] for similar analyses. The outline of the section is as follows:

1. Express ACQL as a stochastic approximation algorithm [53, 60].
2. Show that Q^c and Q^r converge to an optimal fixed point for any fixed safety discount factor $\gamma_c \in (0, 1)$.
3. Restate our Proposition 1 and prove it by showing that as $\gamma_c \to 1$, Q^r and Q^c converge to the optimal state-action value function Q^{r*} and its corresponding optimal (undiscounted) state-action safety function Q^{c*}.

A.1 Setup

Assumption 1. *The augmented CMDP $\mathcal{M}^A = (\mathcal{S}^A, \mathcal{A}, \mathcal{T}^A, d_0^A, r^A, c^A, \gamma, \mathcal{L})$ for ACQL is defined on a finite state space $\mathcal{S}^A$ and action space $\mathcal{A}$. For every state $s \in \mathcal{S}^A$ and action $a \in \mathcal{A}$, there is an associated bounded deterministic reward $r_{sa} = r^A(s, a)$ and bounded constraint feedback $c_{sa} = c^A(s, a)$ observed if action a is applied at state s.*

Under Assumption 1, Q^c and Q^r are vectors in $\mathbb{R}^d$ where $d = |\mathcal{S}^A \times \mathcal{A}|$ is finite. The ACQL algorithm can be modeled as a distributed, asynchronous series of noisy updates to components of Q^c and Q^r.

Assumption 2. *For each state-action pair $(s, a) \in \mathcal{S}^A \times \mathcal{A}$, there are an infinite number of updates applied to the components $Q^r_{s,a}$ and $Q^c_{s,a}$.*

The updates to these components are given by

$$Q^c_{s,a}(n+1) = Q^c_{s,a}(n) + a(n)\left[\Big((1-\gamma_c)c_{sa} + \gamma_c \min\{c_{sa}, \bar{Q}^c_{s',\pi(s')}(n)\}\Big) - Q^c_{s,a}(n)\right] \text{ and} \tag{5}$$

$$Q^r_{s,a}(n+1) = Q^r_{s,a}(n) + b(n)\left[(r_{sa} + \gamma \bar{Q}^r_{s',\pi(s')}(n)) - Q^r_{s,a}(n)\right], \tag{6}$$

where s' is a randomly sampled next state following the state s and action a. The elements of $\bar{Q}^c(n)$ and $\bar{Q}^r(n)$ are potentially taken from older iterations $Q^c_{s,a}(\nu_{s,a}(n))$ and $Q^r_{s,a}(\nu_{s,a}(n))$ where $\nu_{s,a}(n)$ is an integer satisfying $0 \leq \nu_{s,a}(n) \leq n$. Recall that the policy π here is defined as $\arg\max_{a:\bar{Q}^c_{s,a} > \mathcal{L}} \bar{Q}^r_{s,a}$ in terms of $\bar{Q}^c$ and $\bar{Q}^r$. However, we assume that old information is eventually discarded as $n \to \infty$.

Assumption 3. *For all (s, a), $\lim_{n\to\infty} \nu_{s,a}(n) = \infty$.*

Assumption 3 is necessary to prove the convergence of distributed asynchronous stochastic approximation algorithms using outdated values ($\bar{Q}^c$ and $\bar{Q}^r$) [60, 61]. Using $\bar{Q}^c$ is additionally necessary to define the operator in (8) such that a fixed policy π can be used to prove the contraction property in Lemma 1.

We also update γ_c infinitely often with

$$\gamma_c(n+1) = \gamma_c(n) + c(n)\left[(1 - \gamma_c(n)) - \gamma_c(n)\right]. \tag{7}$$

and assume that its updates are synchronized with the index n for the updates to the components of Q^c and Q^r.

Assumption 4. *The step sizes $a(n)$, $b(n)$, and $c(n)$ for the above updates satisfy*

$$\sum_{n=0}^{\infty} a(n) = \sum_{n=0}^{\infty} b(n) = \sum_{n=0}^{\infty} c(n) = \infty$$

$$\sum_{n=0}^{\infty} a(n)^2, \sum_{n=0}^{\infty} b(n)^2, \sum_{n=0}^{\infty} c(n)^2 < \infty,$$

$b(n) \in o(a(n))$, and $c(n) \in o(b(n))$.

Now, let $g : \mathbb{R}^d \times \mathbb{R}^d \times \mathbb{R} \to \mathbb{R}^d$ and $h : \mathbb{R}^d \times \mathbb{R}^d \times \mathbb{R} \to \mathbb{R}^d$ be operators defined for each component (s, a) as

$$g_{s,a}(Q^r, Q^c, \gamma_c) = (1 - \gamma_c)c_{sa} + \gamma_c \mathop{\mathbb{E}}_{s'} \left[\min\{c_{sa}, Q^c_{s',\pi(s')}\} \right] \tag{8}$$

$$h_{s,a}(Q^r, Q^c, \gamma_c) = r_{sa} + \gamma \mathop{\mathbb{E}}_{s'} \left[Q^r_{s',\pi(s')} \right]. \tag{9}$$

Define a third mapping $f(Q^r, Q^c, \gamma_c) = 1 - \gamma_c$. Without loss of generality, we express all the operators as mappings from $\mathbb{R}^d \times \mathbb{R}^d \times \mathbb{R}$ to consider them as a coupled mapping from $\mathbb{R}^{2d+1}$ to $\mathbb{R}^{2d+1}$. Finally, define two martingale difference sequences

$$M^c_{s,a}(n+1) = \gamma_c \min\{c_{sa}, \bar{Q}^c_{s',\pi(s')}(n)\} - \gamma_c \mathop{\mathbb{E}}_{s'} \left[\min\{c_{sa}, \bar{Q}^c_{s',\pi(s')}(n)\} \right] \text{ and} \tag{10}$$

$$M^r_{s,a}(n+1) = \gamma \bar{Q}^r_{s',\pi(s')}(n) - \gamma \mathop{\mathbb{E}}_{s'} \left[\bar{Q}^r_{s',\pi(s')}(n) \right]. \tag{11}$$

The updates to γ^c are deterministic. Using the above, we can express the three ACQL updates (5), (6), and (7) as

$$Q^c_{s,a}(n+1) = Q^c_{s,a}(n) + a(n) \left[g_{s,a}(\bar{Q}^r(n), \bar{Q}^c(n), \gamma_c(n)) - Q^c_{s,a}(n) + M^c_{s,a}(n+1) \right], \tag{12}$$

$$Q^r_{s,a}(n+1) = Q^r_{s,a}(n) + b(n) \left[h_{s,a}(\bar{Q}^r(n), \bar{Q}^c(n), \gamma_c(n)) - Q^r_{s,a}(n) + M^r_{s,a}(n+1) \right], \tag{13}$$

$$\gamma_c(n+1) = \gamma_c(n) + c(n) \left[f(Q^r(n), Q^c(n), \gamma_c(n)) - \gamma_c(n) \right]. \tag{14}$$

Under the above assumptions and formulation, ACQL can now be analyzed as a distributed stochastic approximation algorithm under three timescales.

A.2 Convergence of Q^r and Q^c under a fixed γ_c

Since the update to γ_c happens much more slowly than the updates to Q^r and Q^c—formally, the step size $c(n)$ for γ_c shrinks faster than both $b(n)$ and $a(n)$—we can treat γ_c as approximately fixed while analyzing the behavior of Q^r and Q^c. This allows us to study the convergence of Q^r and Q^c assuming that γ_c is a constant value in the interval $(0, 1)$.

Lemma 1. *The mapping $g^c = g(Q^r, \cdot, \gamma_c) : \mathbb{R}^d \to \mathbb{R}^d$, for some fixed Q^r, some fixed feasible policy π (e.g., a policy based on $\bar{Q}^c$ and $\bar{Q}^r$ as in ACQL), and $\gamma_c \in (0, 1)$, is a contraction mapping.*

Proof.

$$\begin{aligned}
|g^c(Q^c)_{s,a} - g^c(\hat{Q}^c)_{s,a}| &= |\gamma_c \mathop{\mathbb{E}}_{s'} \left[\min\{c_{sa}, Q^c_{s',\pi(s')}\} \right] - \gamma_c \mathop{\mathbb{E}}_{s'} \left[\min\{c_{sa}, \hat{Q}^c_{s',\pi(s')}\} \right]| \\
&= \gamma_c \mathop{\mathbb{E}}_{s'} \left[|\min\{c_{sa}, Q^c_{s',\pi(s')}\} - \min\{c_{sa}, \hat{Q}^c_{s',\pi(s')}\}| \right] \\
&\leq \gamma_c \mathop{\mathbb{E}}_{s'} \left[|Q^c_{s',\pi(s')} - \hat{Q}^c_{s',\pi(s')}| \right] \quad (|\min\{a, b\} - \min\{a, c\}| \leq |b - c|) \\
&\leq \gamma_c ||Q^c - \hat{Q}^c||_\infty
\end{aligned}$$

Therefore, $||g^c(Q^c) - g^c(\hat{Q}^c)||_\infty \leq \gamma_c ||Q^c - \hat{Q}^c||_\infty$. □

Lemma 2. *As $n \to \infty$, $Q^c(n)$ converges to a fixed point $\lambda_1(Q^r, \gamma_c)$ for some fixed Q^r and γ_c.*

Proof. The convergence of Q^c for a fixed Q^r and γ_c follows from Theorem 3 (convergence of distributed stochastic approximation algorithms for a contraction mapping) in [60]. Assumptions 1, 2, and 3 in [60] are satisfied due to our Assumptions 3, 4 and the definitions of $M^c_{s,a}$, $M^r_{s,a}$ in (10) and (11). Furthermore, the contraction property of g^c (Lemma 1) is enough to satisfy Assumption 5 in [60]. Under these conditions, Theorem 3 in [60] holds true. □

Lemma 3. *As $n \to \infty$, $Q^r(n)$ updated with* (13) *using a fixed $Q^c(n) = \lambda_1(Q^r(n), \gamma_c)$, such that there is a feasible action in every state, converges to the optimal value function $Q^{r^*}_{\gamma_c}$.*

Proof. The mapping $h^r = h(\cdot, Q^c, \gamma_c) : \mathbb{R}^d \to \mathbb{R}^d$ for a fixed $Q^c = \lambda(Q^r, \gamma_c)$ is a typical Bellman operator for a fixed policy using only actions from a constant non-empty subset of $\mathcal{A}$ for each state s. As a result, Theorem 4 (convergence of standard Q-learning) in [60] applies. □

Lemma 4. *$Q^r(n)$ and $Q^c(n)$ asymptotically approach $Q^{r^*}_{\gamma_c}$ and $Q^{c*}_{\gamma_c} = \lambda_1(Q^{r^*}_{\gamma_c}, \gamma_c)$ as $n \to \infty$.*

Proof. Lemmas 2 and 3 serve to satisfy Assumptions 1 and 2 in Chapter 6 of [53]. The boundedness of our rewards and constraint signals also result in a bounded $Q^r(n)$ and $Q^c(n)$, which satisfies Assumption 3 in Chapter 6 of [53]. The proof follows from Theorem 2 (convergence of two-timescale coupled stochastic approximation algorithms) in the same chapter. □

A.3 Convergence of (Q^r, Q^c) and γ_c

We can apply a similar two-timescale argument now using γ_c on the slower timescale and $(Q^r(n), Q^c(n))$ on the faster timescale. The condition that the faster timescale converges to a fixed point $\lambda_2(\gamma_c)$ for a static γ_c is shown in Lemma 4. For the condition that the slower timescale converges to a fixed point with $(Q^r(n), Q^c(n)) = \lambda_2(\gamma_c))$ is true trivially because γ_c converges without depending on $(Q^r(n), Q^c(n))$ at all.

Lemma 5. *γ_c converges to 1 as $n \to \infty$.*

Proof. The update in (14) is a discretization of the ODE $\dot{\gamma_c}(t) = 1 - \gamma_c(t)$. The solution to this ODE is $\gamma_c(t) = 1 - (1 - \gamma_c(0))e^{-t}$, which asymptotically approaches 1 as $t \to \infty$. □

Finally, similar to Proposition 1 in [16], we observe that $\lim_{\gamma_c \to 1} g^c_{s,a}(Q^c) = \min\{c_{sa}, \mathbb{E}_{s'} Q^c_{s',\pi(s')}\}$ yields a fixed point at $Q^{c*}_{s,a} = \mathbb{E}_{\tau\sim\pi}\left[\min_{t\in[0,\infty]} c_{sa_t} | s_0 = s, a_0 = a\right]$ matching the undiscounted minimum-safety constraint (Equation (2) in our main paper). Using this fact and another application of Theorem 2 in [53], we can prove our Proposition 2.

Proposition 2. *Let $\mathcal{M}^{\mathcal{A}}$ be an augmented CMDP with $|\mathcal{S}^A| < \infty$, $|\mathcal{A}| < \infty$, and $\gamma \in [0, 1)$, and let $Q^c(n)$ and $Q^r(n)$ be models for the state-action safety and value functions indexed by n. Assume they are updated using Robbins-Monro step sizes $a(n)$ and $b(n)$, respectively, with $b(n) \in o(a(n))$ according to* (5) *and* (6)*. Assume that $\gamma_c(n)$ is also updated with step sizes $c(n)$ such that $\gamma_c(n) \to 1$ and $c(n) \in o(b(n))$. Then $Q^c(n)$ and $Q^r(n)$ converge to Q^{c*} and Q^{r*} almost surely as $n \to \infty$.*

Proof. By Theorem 2 from Chapter 6 of [53], whose conditions are satisfied by Lemmas 4 and 5, the coupled iterates $(\gamma_c(n), Q^r(n), Q^c(n))$ converge almost surely to a fixed point $(1, \lambda_2(1))$ with $\lambda_2(\gamma_c) = (Q^{r*}_{\gamma_c}, \lambda_1(Q^{r*}_{\gamma_c}, \gamma_c))$ as $n \to \infty$. As $\gamma_c \to 1$, $Q^c(n) = \lambda_1(Q^{r*}_{\gamma_c}, \gamma_c)$ also converges to $\mathbb{E}_{\tau\sim\pi}\left[\min_{t\in[0,\infty]} c_{sa_t} | s_0 = s, a_0 = a\right]$ with the policy π determined by $\lim_{n\to\infty} \bar{Q}^r(n) = Q^{r*}$. Therefore, the algorithm attains the optimal state-action value function and the corresponding optimal (undiscounted) state-action safety function Q^{c*}. □

B Additional ACQL Details and Pseudocode

Automaton Analysis To better illustrate the initial automaton analysis in ACQL (Line 2), consider the automaton in Figure 5. There is only one non-accepting sink-components of this automaton, and it is the component consisting of the single node q_3. For q_0, there is only one transition into this component via the edge labeled by p_4, so the safety for q_0 condition is $S(q_0) = \neg p_4$. For q_1 and q_2, there are no transitions to a non-accepting sink-component and so their safety conditions are $S(q_1) = S(q_2) = 1$, meaning that the safety condition is trivially satisfied at all times in those states. For completeness, we also consider the unsafe states themselves as having safety conditions equal to the conjunction of their negated incoming transitions. Therefore, q_3 also has the safety condition $S(q_3) = \neg p_4$.

Now we can obtain the liveness constraints, which are summarized in the liveness condition mapping $O : \mathcal{Q} \to \Phi$ (See Section 4.1 in our main paper). For q_0, the only remaining outgoing edge is the one labeled $\neg(p_1 \vee p_2) \wedge \neg p_4$. Since $S(q_0) = \neg p_4$, we can eliminate it from this transition predicate to obtain $O(q_0) = (p_1 \vee p_2)$. For q_1, one can simply obtain $O(q_1) = p_3$ from its only outgoing edge. For completeness, we also set $O(q_2) = p_3$ using the incoming edges for q_2 since it is an

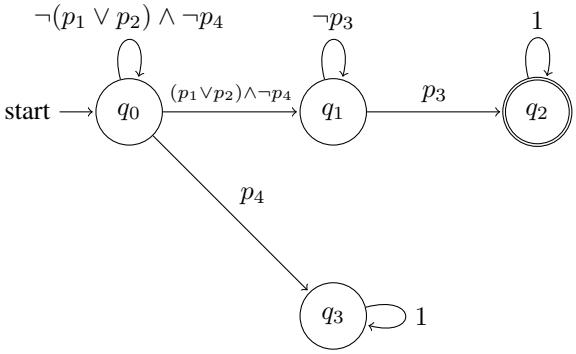

Figure 5: Automaton for the task "Reach goal g_1 or g_2 while never entering an unsafe-region u_1. Then reach g_3.", where achieving the goal g_i corresponds to the atomic proposition p_i and entering u_1 corresponds to p_4. The full LTL expression is $\neg p_4 \; \mathcal{U} \; ((p_1 \vee p_2) \wedge \circ \Diamond p_3)$. The proposition p_4 is only relevant to the task's safety constraint, and the propositions p_1, p_2, and p_3 are only relevant to the task's liveness constraints.

accepting state. This is purely to inform the agent of the goal associated with an accepting state once it has reached it. From the above values for O, the mapping G can be defined by $G(q_0) = \{g_1, g_2\}$, $G(q_1) = \{g_3\}$ and $G(q_2) = \{g_3\}$.

Subroutines Algorithms 2, 3, and 4 present the pseudo-code for collecting trajectories in $\mathcal{M}^A$, relabeling them with achieved goals, and computing the safety discount factor γ_c.

The GetTrajectory function, in Algorithm 2, begins by sampling an initial state from the distribution d_0^A. We also randomly sample positions from the environment to associate with each subgoal proposition $p \in AP_{\text{subgoal}}$. This task randomization promotes collecting trajectories that explore a greater portion of the state space through a variety of subgoal sequences, and we found that this was necessary to stabilize training while using HER. We speculate that the greater variety of state and subgoal combinations is needed to train a robust subgoal-reaching policy. The agent proceeds to interact with the environment for a total of T steps. In a loop indexed by t, actions are selected from an epsilon-greedy version of the input policy π (Line 5). The reward, constraint feedback, and next state are observed (Lines 6-8) and stored in the trajectory τ (Line 9). After T steps have executed, the trajectory is returned.

The Relabel function, in Algorithm 3, takes a batch of trajectories $\mathcal{B}_\tau$. For each trajectory in the batch, the function determines the final achieved state g' and overwrites a single subgoal for every step in the entire trajectory with g'. It also overwrites the reward for each step with 1 for steps that were sufficiently close to g' and 0 for steps that were not. We found that this relatively simple strategy, despite the fact that trajectories were collected with multiple-subgoals in-mind, was sufficient to train reliable goal-reaching policies.

The SafetyGammaScheduler function, in Algorithm 4, generates values for γ_c, starting from an initial value and gradually increasing toward 1.0 with exponential decay. To ensure accurate learning of state-action safety function models, it was necessary to cap γ_c at a value slightly below 1.0.

C Model Architectures, Environment Implementation Details, and Hyper-Parameters

Model Architecture and Policy Our method trains two models: the state-action value function, Q_ψ^r, and the state-action safety function, Q_θ^c. Both models employ twin neural networks and use the minimum of their predicted values to mitigate overestimation in value and safety estimation. For the ablation study using a state-action sum-of-costs function, we likewise use twin networks, but instead take the maximum of the two predictions to maintain a conservative (i.e., pessimistic) estimate.

To simplify handling multiple goals, Q_ψ^r is defined using a goal-conditioned state-action value function model, $Q_\psi^{GC} : \mathcal{S} \times \mathcal{G} \times \mathcal{Q} \times \mathcal{A} \to \mathbb{R}$, parameterized by ψ. At runtime, Q_ψ^{GC} is called for

Algorithm 2 GetTrajectory

function GETTRAJECTORY($\mathcal{M}^A$, π)
  $s_0^A \sim d_0^A$, $g_i \sim P(\mathcal{G})$ for $p_i \in AP_{\text{subgoals}}$
  $t \leftarrow 0$, $\tau \leftarrow ()$
  while $t < T$ **do**
    $a_t \sim \pi_{\epsilon-\text{greedy}}(s_t^A)$
    $r_t \leftarrow r^A(s_t^A, a_t)$
    $c_t \leftarrow c^A(s_t^A, a_t)$
    $s_{t+1}^A \sim \mathcal{T}^A(s_t^A, a_t)$
    $\tau \leftarrow \tau \cup (s_t^A, r_t, c_t, a_t)$
    $t \leftarrow t + 1$
  end while
  return τ
end function

Algorithm 3 Relabel

function RELABEL($\mathcal{B}_r$)
  for $\tau \in \mathcal{B}_r$ **do**
    $g' \leftarrow$ the final goal state achieved in τ.
    for $s_t^A, r_t \in \tau$ **do**
      Replace g_1 in s_t^A with g'
      $r_t \leftarrow 1$ if g' achieved in s_t^A and 0 otherwise.
    end for
  end for
  return $\mathcal{B}_r$
end function

each subgoal $g \in g^+$. This approach exploits the fact that goal-conditioned value functions form a Boolean algebra under the $\min$ and $\max$ operators [21, 34]. For example, consider two subgoal propositions $p_1, p_2 \in AP_{\text{subgoal}}$. In the simplest case, when $O(q) = p_1$, we compute $Q_\psi^r(\langle s, g_1, q\rangle, a)$ as $Q_\psi^{GC}(s, g_1, q, a)$. When $O(q) = p_1 \wedge p_2$ (i.e., both subgoals must be achieved to progress), we compute the value as the minimum of $Q_\psi^{GC}(s, g_1, q, a)$ and $Q_\psi^{GC}(s, g_2, q, a)$. Conversely, when $O(q) = p_1 \vee p_2$ (i.e., achieving either subgoal suffices), the value is the maximum of $Q_\psi^{GC}(s, g_1, q, a)$ and $Q_\psi^{GC}(s, g_2, q, a)$. This pattern generalizes to arbitrarily complex Boolean formulae, allowing us to efficiently approximate Q_ψ^r using a single goal-conditioned network.

We also observed that, because liveness constraints are separated into the goal input, conditioning behavior on the automaton state is only necessary when safety constraints differ between automaton states. As a result, we do not require a distinct "mode" for every automaton state $q \in \mathcal{Q}$, but only for each unique safety condition in the mapping S. To encode this, we train Q_ψ^r using a multi-headed neural network, where each output head corresponds to a distinct safety condition. For example, in the automaton shown in Figure 5, the mapping S assigns states to one of two safety conditions: $\neg p_4$ or 1. Accordingly, Q_ψ^{GC} has two output heads, selected based on the currently active safety condition. In all ACQL experiments, Q_ψ^{GC} shared a hidden layer of 256 neurons across all heads; each head then had an additional hidden layer of 256 neurons. All layers used ReLU activations, and the final output layer had $|\mathcal{A}|$ neurons with no activation function.

The model Q_θ^c follows the same architecture as Q_ψ^r, with a goal-conditioned, multi-headed neural network, but differs in two key respects. First, for disjunctive goal conditions ($p_1 \vee p_2$), the output is defined as the minimum of $Q_\theta^{GC}(s, g_1, q, a)$ and $Q_\theta^{GC}(s, g_2, q, a)$, to ensure conservative safety by taking the worst-case estimate across disjunctive paths. Second, Q_θ^{GC} uses a different network architecture: it has two shared hidden layers of 64 neurons each, and each output head includes two additional hidden layers with 64 and 32 neurons, respectively. All layers use ReLU activations. The final output layer consists of $|\mathcal{A}|$ neurons with a $\tanh$ activation function.

The policy was implemented in terms of these two value functions according to the constrained maximization $\pi(s) = \arg\max_{a: Q_\theta^c(s,a) > \mathcal{L}} Q_\psi^r(s, a)$. In the case that no action was deemed feasible by Q_θ^c, the safest action $\max_a Q^c(s, a)$ was chosen. The exploration policy $\pi_{\epsilon-\text{greedy}}$ would behave

Algorithm 4 SafetyGammaScheduler

function SAFETYGAMMASCHEDULER(j)
  x $\leftarrow j \div$ update_period
  y $\leftarrow 1.0 - (1.0 - \text{init\_value}) \cdot \text{decay\_rate}^{\text{x}}$
  return $\begin{cases} \text{max\_value} & \text{if y} \geq \text{max\_value} \\ \text{y} & \text{o.w.} \end{cases}$
end function

as above with probability $1 - \epsilon$, and with probability ϵ select a random action without considering Q^r or Q^c.

Environment Implementation For our simulated experiment environments, we used the Brax physics simulator [57] and assets provided in JaxGCRL [62] for the PointMass, Quadcopter, and Ant environments. Acting in these environments was facilitated by a set of discrete actions corresponding to movement in the cardinal directions. Specifically, the actions in the PointMass and Quadcopter environments output a constant low-level action to accelerate in one of the four or six available directions for 5 consecutive steps. The actions for our UR5e environment, which we used to train our real-world-deployed policies, similarly moved the robot's end effector in the 6 cardinal directions for a single time step. The actions in the AntMaze environment were policies trained separately using Proximal Policy Optimization (PPO) [7] for 50000000 environment interactions with the objective of maximizing velocity in each of the four cardinal directions and would run for 4 consecutive steps when executed. All further details regarding environment geometry and task definitions for our simulated and real-world experiments are included in our Anonymized Code Repository[1].

Hyper-Parameters Table 3 reports the hyperparameter values most commonly used in our experiments, including hyperparameters for the safety gamma (γ_c) scheduler described in Appendix B. For a complete account of hyperparameters, as well as ACQL, baseline, and environment implementation details, refer to our Anonymized Code Repository[2]1.

Table 3: Hyperparameter values used for experiments in Tables 1 and 2 in our main paper

Hyperparameter Name	Value
Episode length (T)	1000
Discount factor (γ)	0.99
Learning rate (α)	$1 \cdot 10^{-4}$
ϵ-greedy factor (ϵ)	0.1
Safety limit ($\mathcal{L}$)	0.0
Safety Gamma Init Value	0.80
Safety Gamma Update Period	$250,000$
Safety Gamma Decay Rate	0.15
Safety Gamma Max. Value	0.98
Target parameter interpolation factor (λ)	0.005

Compute Resource Requirements All experiments were conducted on a single NVIDIA RTX 3090 GPU (24 GB VRAM), using a local workstation equipped with an 12th Gen Intel i7-12700F CPU, 32 GB RAM. No cloud services or compute clusters were used. Each individual experimental run required approximately 30 minutes of compute time on the GPU. The full experiment grid consists of 225 runs for the comparative analysis and 90 runs for the ablations, amounting to approximately 315 GPU-hours. Minor additional compute was used for initial hyperparameter tuning and development.

D Expanded Experimental Results

Figures 6 and 7 show the average reward and success rate throughout training for the baseline comparison experiments summarized in Table 1. The LOF baseline cannot be depicted on these

[1] https://anonymous.4open.science/r/acql-4B4C

plots as it does not learn a single policy in the same MDP as the other methods, and instead learns a policy that chooses subgoal-specific options for an abstracted state space $\mathcal{Q} \times \mathcal{S}_g$ constructed from the automaton states $\mathcal{Q}$ and the finite set of states $\mathcal{S}_g \subset \mathcal{S}$ corresponding to task subgoals. Figures 8 and 9 show the average reward and success rate throughout training for the experiments summarized in Table 2 in our main paper. The differences in amount of training steps depicted by the figures is due to the different design and training pipelines that the two algorithms observe. ACQL collects complete trajectories to store in the Replay Buffer and CRM-RS just collects individual transitions. We want to highlight that our algorithm converges earlier during the training and this difference does not play a significant role in the performance gap reported in Table 1.

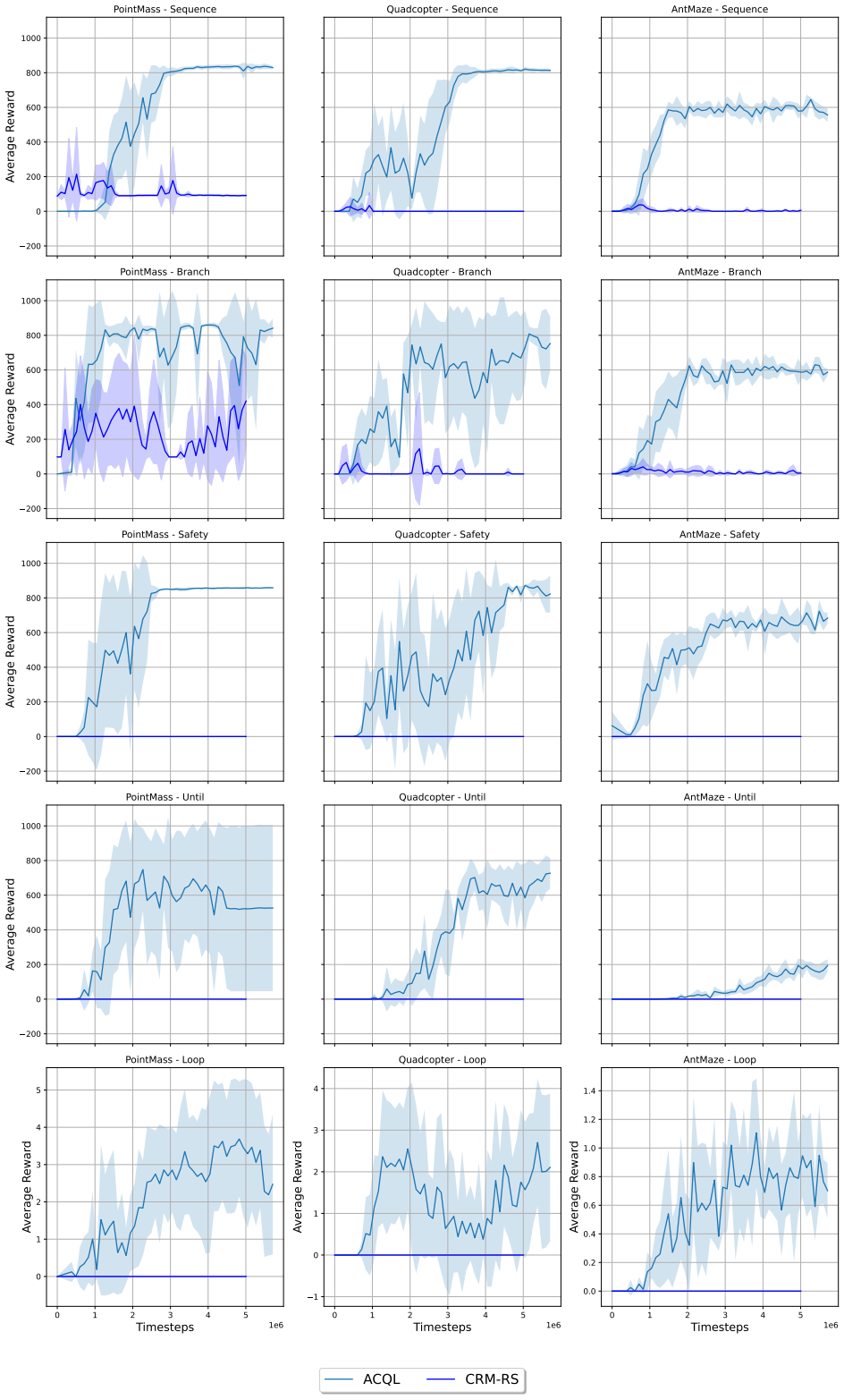

Figure 6: Average and one standard deviation of episode reward throughout training for the five runs per method that are summarized in Table 1 in our main paper.

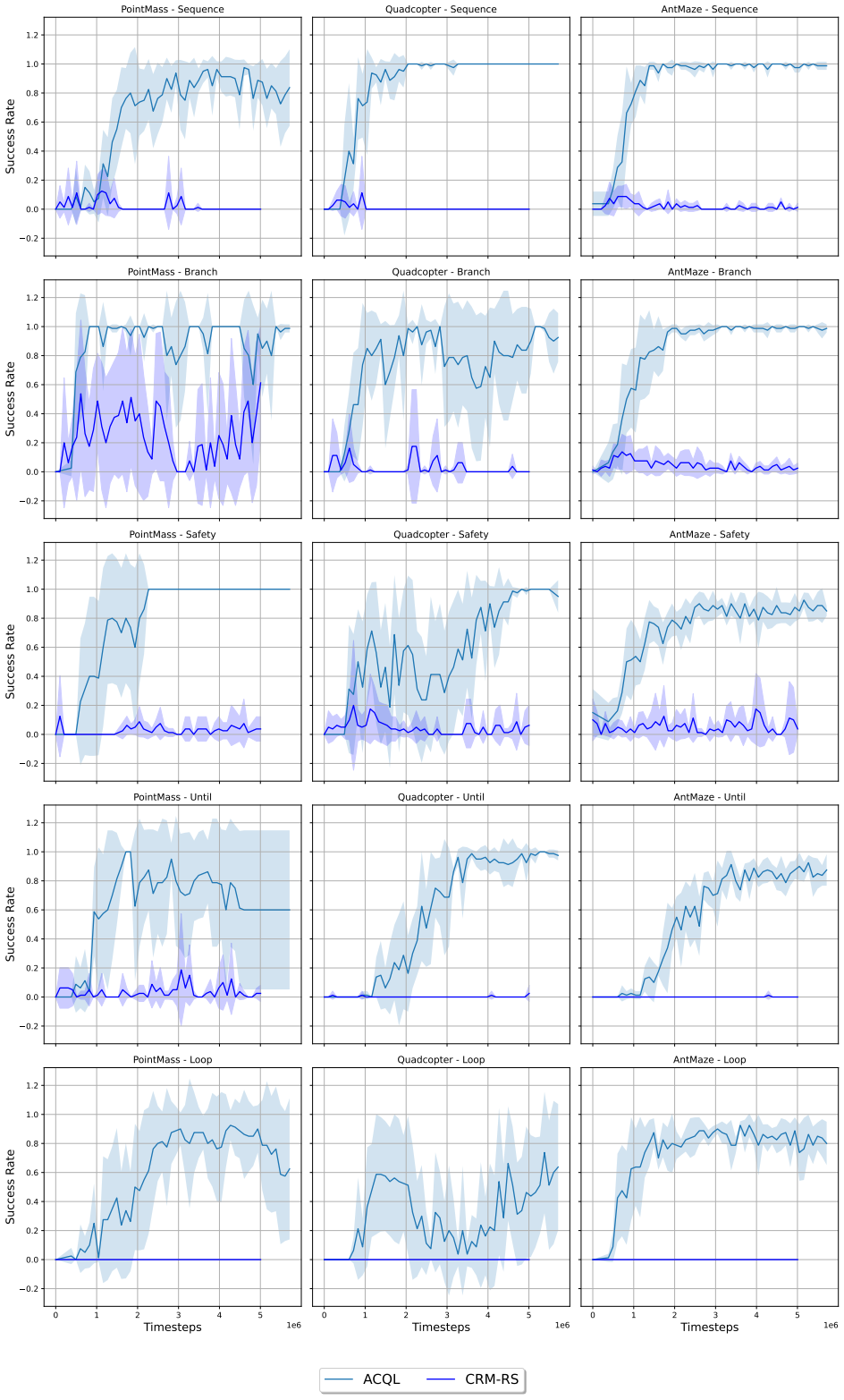

Figure 7: Average and one standard deviation of episode success rate throughout training for the five runs per method that are summarized in Table 1 in our main paper.

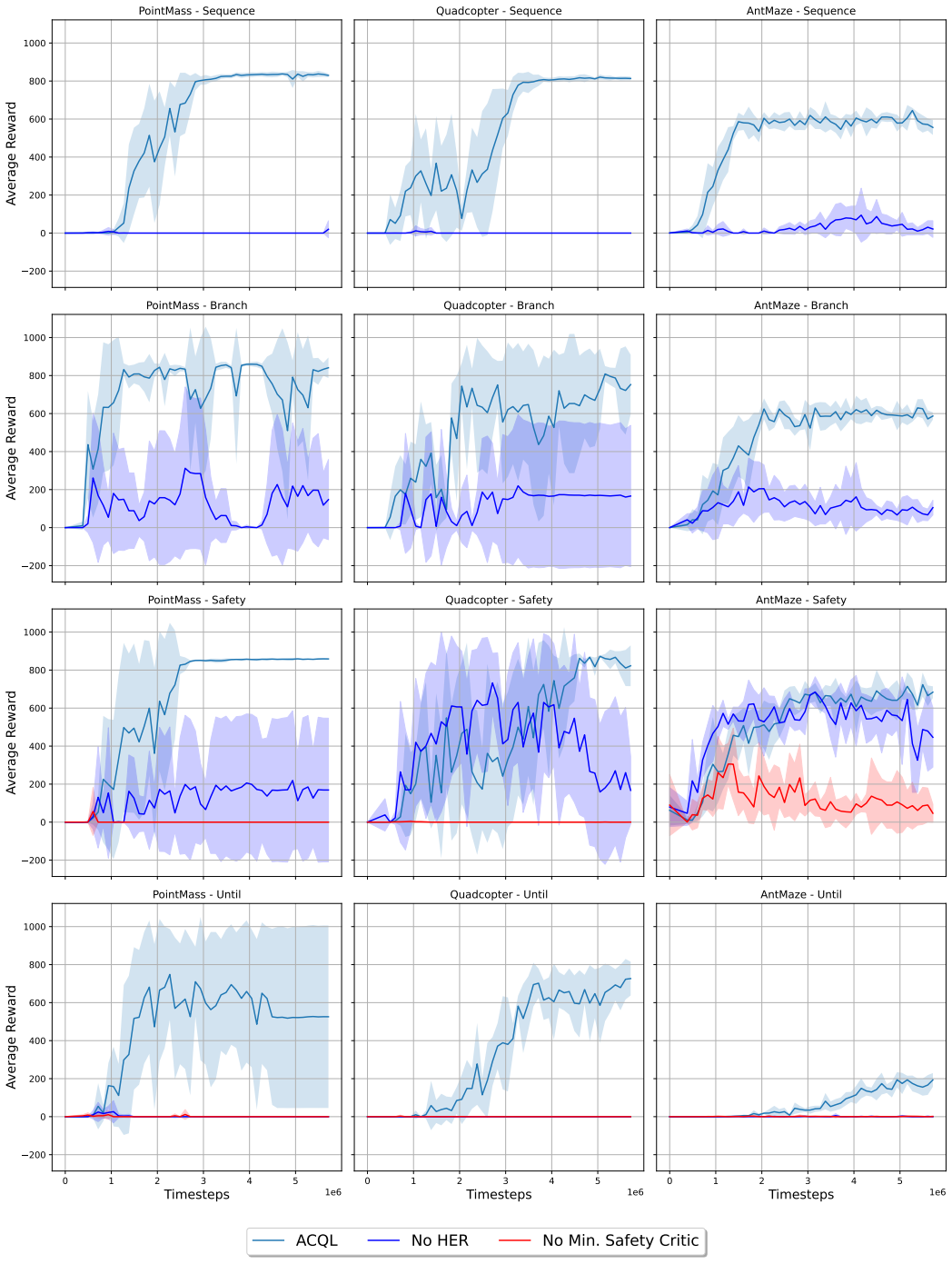

Figure 8: Average and one standard deviation of episode reward throughout training for the five runs per ablation group that are summarized in Table 2 in our main paper.

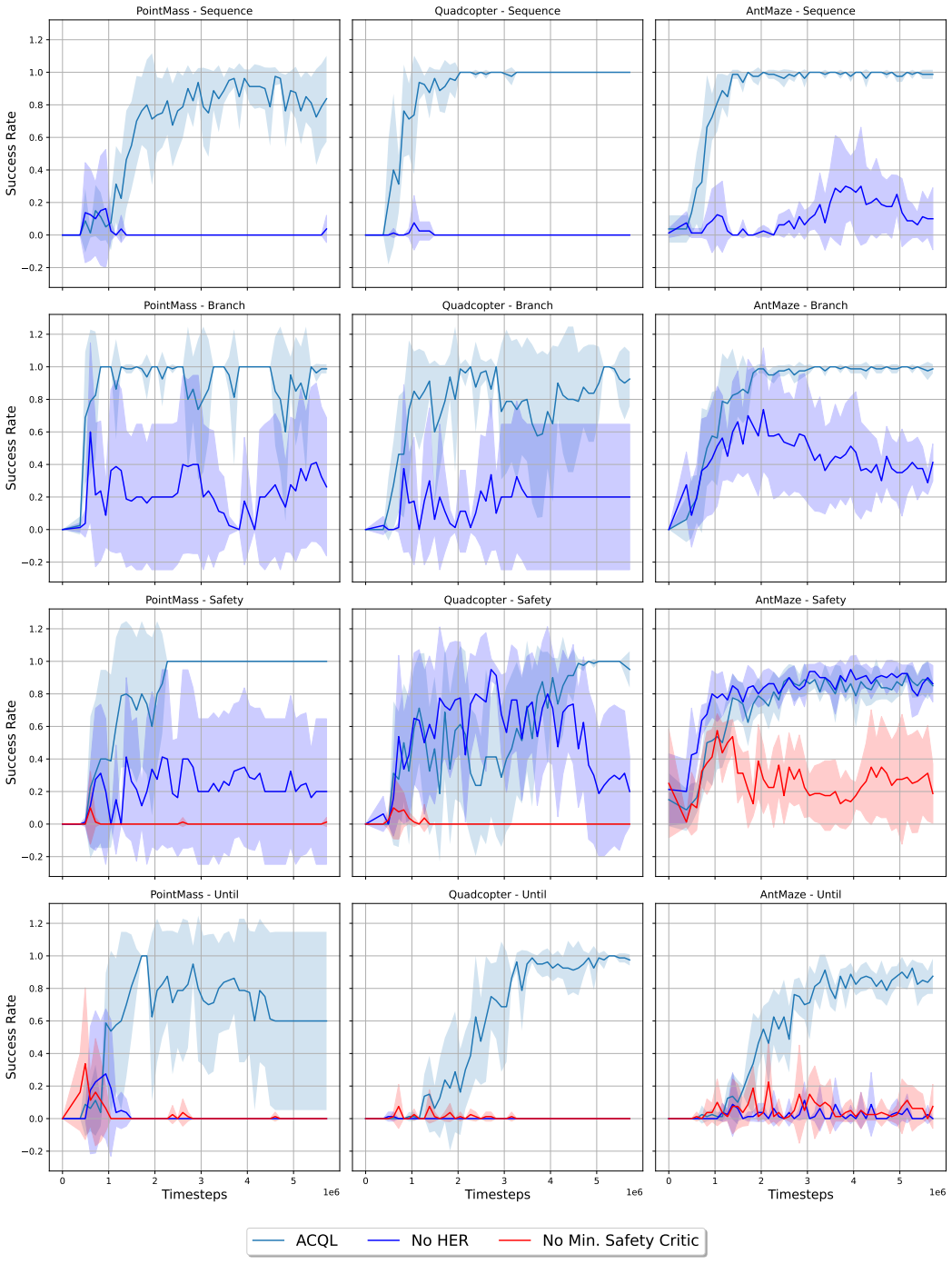

Figure 9: Average and one standard deviation of episode success rate throughout training for the five runs per ablation group that are summarized in Table 2 in our main paper.